

**School of Applied Chemistry**

**Coordination Studies of Inositols with Aluminium and Related  
Cations**

**Davlin M D Chokazinga**

**This thesis is presented for the Degree of  
Master of Science  
of  
Curtin University of Technology**

**December 2003**

## TABLE OF CONTENTS

<b>ABSTRACT</b>	<b>v</b>
<b>ACKNOWLEDGEMENTS</b>	<b>vii</b>
<b>LIST OF TABLES</b>	<b>viii</b>
<b>LIST OF FIGURES</b>	<b>viii</b>
<b>ABBREVIATIONS USED</b>	<b>xii</b>
<b>CHAPTER 1- INTRODUCTION</b>	<b>1</b>
<b>1.1 ALUMINA PRODUCTION</b>	<b>1</b>
1.1.1 Effect of organic compounds on gibbsite precipitation	3
<b>1.2 CYCLITOLS</b>	<b>6</b>
1.2.1 Synthesis of cyclitols	7
1.2.1.1 Permanganate hydroxylation of 1,3-cyclohexanediene	7
1.2.1.2 Diels-Alder synthesis of cyclitols	8
1.2.2 Synthesis of <i>cis</i> -inositol	8
1.2.2.1 Synthesis from <i>epi</i> -inositol	8
1.2.2.2 A simple synthesis of <i>cis</i> -inositol	10
1.2.3 Synthesis of <i>epi</i> -inositol	10
<b>1.3 COORDINATION ABILITIES OF THE INOSITOLS</b>	<b>11</b>
1.3.1 Infrared spectroscopy	12
1.3.2 High performance liquid chromatography	13
1.3.3 NMR coordination studies	14
1.3.4 Paper electrophoresis	19
1.3.5 Ion exchange thin layer chromatography	20
1.3.6 X-ray crystallography	21
<b>1.4 SCOPE OF THIS PROJECT</b>	<b>22</b>
1.4.1 Synthesis of inositols	22
1.4.2 Coordination modalities	22
1.4.3 Coordination trends under basic conditions	23
<b>CHAPTER 2- EXPERIMENTAL PROCEDURES</b>	<b>24</b>
<b>2.1 GENERAL EXPERIMENTAL DETAILS</b>	<b>24</b>
2.1.1 Nuclear magnetic resonance (NMR) spectra	24
2.1.2 Infrared (IR) spectra	24
2.1.3 High performance liquid chromatography (HPLC)	24

<b>2.2</b>	<b>CHEMICALS AND MATERIALS USED</b>	<b>25</b>
<b>2.3</b>	<b>SYNTHESES</b>	<b>26</b>
2.3.1	Tetrahydroxyquinone	26
2.3.2	Synthesis of <i>epi</i> -inositol	27
2.3.3	Synthesis of <i>cis</i> -inositol from tetrahydroxyquinone	28
2.3.3.1	Isolation of <i>cis</i> -inositol via isopropylidenation	29
2.3.3.2	Purification of <i>cis</i> -inositol	31
2.3.4	Synthesis of <i>myo</i> -inositol carbonate	31
2.3.4.1	Purification of the orthoformate derivative	32
2.3.4.2	Introduction of the silyl ether group	33
2.3.4.3	Formation of the protected <i>myo</i> -inositol carbonate	33
2.3.4.4	Hydrolysis of substituents groups	35
<b>2.4</b>	<b>PREPARATION OF SOLUTIONS FOR COORDINATION STUDIES</b>	<b>36</b>
2.4.1	Ligand Solutions for NMR Studies	36
2.4.2	Cation solutions	36
2.4.3	Sodium aluminate solution	36
2.4.4	NMR Complexation Ratios	36
<b>2.5</b>	<b>THIN LAYER ION EXCHANGE CHROMATOGRAPHY</b>	<b>37</b>
<b>CHAPTER 3</b>	<b>- RESULTS AND DISCUSSION</b>	<b>38</b>
<b>3.1</b>	<b>SYNTHESES</b>	<b>38</b>
3.1.1	Synthesis of <i>epi</i> -inositol	38
3.1.2	Synthesis of <i>cis</i> -inositol	38
3.1.3	Synthesis of <i>myo</i> -inositol carbonate	39
<b>3.2</b>	<b>ASSIGNMENT OF THE <sup>13</sup>C RESONANCES OF THE INOSITOLS</b>	<b>40</b>
<b>3.3</b>	<b>COORDINATION STUDIES</b>	<b>41</b>
3.3.1	Complexation studies by ion Exchange Chromatography	41
3.3.2	Complexation studies by HPLC	42
3.3.3	<sup>13</sup> C NMR Coordination studies of <i>epi</i> -inositol	43
3.3.3.1	Complexation of <i>epi</i> -inositol with calcium ions	43
3.3.3.2	Complexation of <i>epi</i> -inositol with aluminium ions	45
3.3.3.3	Complexation of <i>epi</i> -inositol with gallium ions	46
3.3.3.4	Complexation of <i>epi</i> -inositol with lanthanum ions	47
3.3.3.5	Complexation of <i>epi</i> -inositol with aluminate anions	50
3.3.4	<sup>13</sup> C NMR Complexation studies of <i>myo</i> -inositol	52
3.3.4.1	Complexation of <i>myo</i> -inositol with calcium ions	53
3.3.4.2	Complexation of <i>myo</i> -inositol with aluminium ions	54
3.3.4.3	Complexation of <i>myo</i> -inositol with Gallium ions	56
3.3.4.4	Complexation of <i>myo</i> -inositol with lanthanum ions	57
3.3.4.5	Complexation of <i>myo</i> -inositol with aluminate anion	58
3.3.5	<sup>13</sup> C NMR Complexation Studies of <i>cis</i> -Inositol	59
3.3.5.1	Coordination of <i>cis</i> -inositol with calcium ions	59
3.3.5.2	Complexation of <i>cis</i> -inositol with aluminium ions	62
3.3.5.3	Complexation of <i>cis</i> -inositol with lanthanum ions	63
3.3.6	<sup>13</sup> C NMR Complexation studies of <i>myo</i> -inositol carbonate	65
3.3.6.1	Complexation of <i>myo</i> -inositol carbonate with calcium ions	65
3.3.6.2	Complexation of <i>myo</i> -inositol carbonate with aluminium ions	66
3.3.6.3	Complexation of <i>myo</i> -inositol carbonate with lanthanum ions	67
3.3.6.4	Complexation of <i>myo</i> -inositol carbonate with samarium ions	68

3.4	SUMMARY OF COORDINATION STUDIES BY $^{13}\text{C}$ NMR SPECTROSCOPY.	70
3.5	TRENDS OF POSSIBLE COMPLEXATION SITES.	70
	CHAPTER 4 - CONCLUSIONS	72
4.2	FURTHER WORK	74
	REFERENCES	76
	APPENDICES	80

## ABSTRACT

In this work *cis*-inositol, *epi*-inositol and *myo*-inositol carbonate were successfully synthesised and used for coordination studies. The preparation of *cis*-inositol was achieved by reduction of tetrahydroxybenzoquinone via hydrogenation with palladium hydroxide as the catalyst and was purified by chromatographic separation using Dowex resin. The synthesis of *epi*-inositol was achieved by the nitric acid oxidation of *myo*-inositol to form *epi*-inosose which was subsequently reduced by hydrogenation using palladium hydroxide as the catalyst. *myo*-Inositol was converted into its mono-orthoformate derivative and the equatorial hydroxy group was then protected as a *tertiary*-butyldimethylsilyl ether. The carbonate group was introduced onto this protected inositol and then the protecting groups were removed by acid hydrolysis.

The coordination characteristics of four inositols, viz *cis*-inositol, *epi*-inositol, *myo*-inositol and *myo*-inositol carbonate with calcium, aluminium, gallium, lanthanum and samarium ions have been investigated. Interactions of the aluminate anion with *epi*-inositol and *myo*-inositol in deuterated sodium hydroxide were also investigated. Three methods were used in the study of complexation behaviour of these systems, namely,  $^{13}\text{C}$  NMR spectroscopy, HPLC and ion exchange chromatography.

$^{13}\text{C}$  NMR spectroscopy was found to be most useful for determining possible complexation behaviour of the inositols. Chemical shift changes of the resonance signals in the  $^{13}\text{C}$  NMR spectra on sequential addition of cations to solutions of the inositols at near neutral pH, have led to determination of possible coordination sites of the inositols. In general, large induced chemical shift changes have been interpreted to signify strong cation-inositol interaction at specific hydroxy groups. Triaxial sites of the inositols have shown a preference to coordinate small ions with ionic size of at least 60 pm, smaller ions than this displayed very weak interactions. Likewise large ions (90-100 pm) imparted weak interactions on triaxial sites of the inositols. These large ions coordinated well with the axial-equatorial-axial sites of the inositols although it was observed that calcium ions appeared to form a 2:1

ligand:cation complex with *cis*-inositol at the triaxial site despite being a large cation (100 pm).

The detection of complex formation by HPLC showed a possible formation of very stable complexes of *epi*-inositol complexes with calcium ions. However, a change of refractive index of the solution on sequential addition of the cation may have caused an interference in the results such that direct interpretation was not possible.

Ion exchange chromatography provided the quickest guide on how strongly the inositols interact with a particular cation. However, determination of complex stoichiometry and/or structure was not possible using this technique.

## **ACKNOWLEDGEMENTS**

I wish to express sincere thanks to my supervisors, Dr. Mauro Mocerino and Associate Professor W. van Bronswijk for their tireless encouragement and valuable guidance throughout this project. I very much appreciate their professional support and patience during my difficult moments.

I am very grateful to Emeritus Professor S. J. Angyal of the University of New South Wales for his valuable personal communications on technical matters relating to this project.

Many thanks also go to all the people with whom I came into contact and assisted me in some aspects of this work.

I am indebted to my family, my wife, Gertrude, my daughters, Lyness and Cynthia and my son Davlin Junior who have been supportive in a great many ways during the course of this work.

Surely, financial support from AusAID and the Malawi Government through the Malawi Bureau of Standards is most gratefully acknowledged with many thanks indeed.

## LIST OF TABLES

Table 1:	Alumina world production (Greenwood and Earnshaw, 1997, pp218).	1
Table 2:	Gibbsite inhibition by polyols and their relative electrophoretic mobility	4
Table 3:	Equilibrium constants, $K$ , of D-glucitol calcium complex derived from $^{13}\text{C}$ NMR chemical shifts (Beatie and Kelso 1981)	17
Table 4:	Electrophoretic Relative mobilities of some cyclitols.	19
Table 5:	Ion exchange $R_f$ values, (Angyal and Craig, 1993)	20
Table 6:	Chemicals and materials used	25
Table 7:	Ethyl acetate/petroleum spirit mixture ratios.	30
Table 8:	Coordination ratios	37
Table 9:	Assignments of $^{13}\text{C}$ NMR spectral resonances of inositols. (Angyal and Odier, 1982, shown in parenthesis)	41
Table 10:	$R_f$ values of cis-inositol, myo-inositol, myo-inositol carbonate and epi-inositol on $\text{Ca}^{2+}$ , $\text{La}^{3+}$ and $\text{Al}^{3+}$ ion exchange plates.	41
Table 11:	$^1\text{H}$ NMR chemical shift changes of epi-inositol induced by lanthanum ions (Angyal and Greeves, 1976 shown in parenthesis)	49
Table 12:	Possible complexation sites of inositols	70

## LIST OF FIGURES

Figure 1: Some C2 - C6 alditols	3
Figure 2: C-5 Alditols	4
Figure 3: An MP arrangement of hydroxy groups	5
Figure 4: Diastereoisomers of inositol (Painter, 1996)	6
Figure 5: Permanganate hydroxylation of 1,3 cyclohexanediene	7
Figure 6: Diels-Alder synthesis of cyclitols	8
Figure 7: Synthesis of <i>cis</i> -inositol from <i>epi</i> -inositol (Angyal and Hickman, 1971)	9
Figure 8: Catalytic reduction of tetrahydroxyquinone to <i>cis</i> -inositol	10
Figure 9: Synthesis of <i>epi</i> -inositol (Posternak, 1952)	11
Figure 10: Ax-eq-ax and triaxial coordination sites	12
Figure 11: Structure of muellitol	14
Figure 12: Possible complexation of 1,2,3,4,5/0-cyclohexane-pentol conformation	15
Figure 13: Coordination sites of <i>cis</i> -inositol	15
Figure 14: Scyllo-inositol orthoformate: triaxial site- only site for coordination	16
Figure 15: Ring inversion of 2- <i>deoxy</i> -2 methyl <i>epi</i> -inositol	16
Figure 16: Calcium complex of D-allopyranosyl-D allopyranoside	22
Figure 17: Synthesis of tetrahydroxyquinone	26
Figure 18: Synthesis of <i>epi</i> -inositol	28
Figure 19: Synthesis of <i>cis</i> -inositol	28
Figure 20: Isopropylidenation of <i>cis</i> -inositol	30
Figure 21: Synthesis of <i>myo</i> -inositol mono-orthoformate	32
Figure 22: Synthesis of <i>tertiary</i> -butyldimethylsilylmono-orthoformate- <i>myo</i> -inositol	33
Figure 23: Synthesis of <i>tertiary</i> -butyldimethylsilylmono-orthoformate- <i>myo</i> -inositol carbonate	34
Figure 24: Hydrolysis of <i>tertiary</i> -butyldimethylsilyl- <i>myo</i> -inositol carbonate mono-orthoformate (40)	35
Figure 25: Synthesis of <i>cis</i> -inositol	38
Figure 26: <sup>13</sup> C NMR chemical shift changes of <i>epi</i> -inositol induced by calcium ions	43
Figure 27: Possible coordination of <i>epi</i> -inositol with calcium ions	44
Figure 28: <sup>13</sup> C NMR chemical shifts of <i>epi</i> -inositol on addition of aluminium ions	45

Figure 29: Possible coordination of <i>epi</i> -inositol with aluminium ions	46
Figure 30: $^{13}\text{C}$ NMR chemical shifts changes of <i>epi</i> -inositol induced by gallium ions	47
Figure 31: Possible coordination of <i>epi</i> -inositol with gallium ions	47
Figure 32: $^{13}\text{C}$ NMR chemical shift changes of <i>epi</i> -inositol induced by lanthanum ions.	48
Figure 33: <i>epi</i> -Inositol and 2- <i>C</i> -methyl <i>epi</i> -inositol	49
Figure 34: <i>epi</i> -Inositol coordination with lanthanum ions	50
Figure 35: $^{13}\text{C}$ NMR chemical shift changes of <i>epi</i> -inositol induced by aluminate anion	51
Figure 36: Stable chair conformation of <i>epi</i> -inositol	51
Figure 37: Possible inversion of <i>epi</i> -inositol	52
Figure 38: $^{13}\text{C}$ NMR chemical shifts of <i>myo</i> -inositol induced by calcium ions	53
Figure 39: Possible inversion of <i>myo</i> -inositol	54
Figure 40: $^{13}\text{C}$ NMR chemical shifts changes of <i>myo</i> -inositol induced by aluminium ions	55
Figure 41: $^{13}\text{C}$ NMR chemical shift changes of <i>myo</i> -inositol induced by gallium ions	56
Figure 42: $^{13}\text{C}$ NMR Chemical shift changes of <i>myo</i> -inositol induced by lanthanum ions	57
Figure 43: Possible coordination of <i>myo</i> -inositol with lanthanum ions	58
Figure 44: $^{13}\text{C}$ NMR chemical shift changes of <i>myo</i> -inositol induced by aluminate anion	59
Figure 45: $^{13}\text{C}$ NMR chemical shift changes of <i>cis</i> -inositol induced by calcium ions	60
Figure 46: Possible coordination of <i>cis</i> -inositol with calcium ions	60
Figure 47: Possible <i>cis</i> -inositol: $\text{Ca}^{2+}$ 2:1 interaction	61
Figure 48: Possible 1:1 coordination of <i>cis</i> -inositol with calcium ions	61
Figure 49: $^{13}\text{C}$ NMR chemical shift changes of <i>cis</i> -inositol induced by aluminium ions	62
Figure 50: Possible coordination site of <i>cis</i> -inositol with $\text{Al}^{3+}$ ion	63
Figure 51: $^{13}\text{C}$ NMR chemical shift changes of <i>cis</i> -inositol induced by lanthanum ions	64
Figure 52: Possible coordination of <i>cis</i> -inositol with lanthanum ions	65
Figure 53: $^{13}\text{C}$ NMR chemical shift changes of <i>myo</i> -inositol carbonate induced by calcium ions	66

Figure 54: Possible coordination of myo-inositol carbonate with calcium ions	66
Figure 55: $^{13}\text{C}$ NMR chemical shift changes of myo-inositol carbonate induced by aluminium ions	67
Figure 56: $^{13}\text{C}$ NMR chemical shift changes of <i>myo</i> -inositol carbonate induced by lanthanum ions	68
Figure 57: $^{13}\text{C}$ NMR chemical shift changes of <i>myo</i> -inositol carbonate induced by samarium ions	69
Figure 58: Possible coordination site of <i>myo</i> -inositol carbonate with $\text{Sm}^{3+}$ ions	69

## ABBREVIATIONS USED

ax	axial positions of hydroxy groups in inositols.
$\delta$	chemical shift downfield from the reference standard tetramethylsilane.
eq	equatorial position of hydroxy groups in inositols.
HETCOR	heteronuclear correlation of nuclear magnetic resonance analysis.
$r_i$	ionic radius.
$J_{a,b}$	nuclear spin coupling constant in Hertz, through two or more bonds.
pm	picometer ( $10^{-12}$ of a meter).
$R_f$	retention distance ratio of a compound on a chromatographic plate (distance moved by a compound divided by distance moved by the eluent solvent).

## CHAPTER 1- INTRODUCTION

### 1.1 ALUMINA PRODUCTION

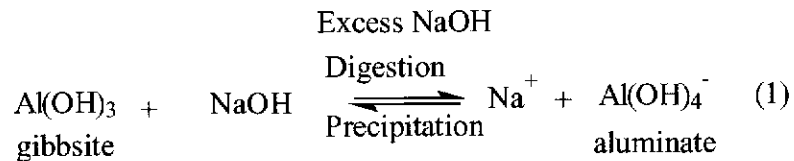
Western Australia has a considerable mineral processing industry in comparison with other States of Australia. One of the minerals being processed on a large scale is alumina, with the current production being 6.8 million tonnes per annum. According to Power, (1991, pp337-345), the estimated production value of alumina in the South-West of Western Australian refineries was AU \$2.34 billion for the fiscal year 1989/1990. This is an outstanding contribution to the national economy, and Australia has been the world's largest producer of alumina for some time (Table 1).

**Table 1: Alumina world production (Greenwood and Earnshaw, 1997, pp218).**

Country	Production (%)
Australia	19.3
USA	17.8
USSR	12.8
Jamaica	8.4
Japan	5.9
Germany	4.7
Canada	4.3
France	4.1

The modern aluminium industry extracts alumina from bauxite ore by the Bayer Process, a distinct four step process, consisting of digestion, clarification, precipitation and calcination. Excess caustic soda is used to solubilise the alumina

during the digestion step to form aluminate ions. Gibbsite crystallisation is achieved by seeding the supersaturated liquor with gibbsite (equation 1). The gibbsite is then calcined at 1200 °C to recover the alumina, (Greenwood and Earnshaw, 1997).



Power (1991) reported that worldwide the Bayer Process is the dominant aluminium extraction technique and to this effect, it is used exclusively in Western Australian alumina refineries. Power further reported that due to the low grade of ore and the presence of a high content of organic material, Western Australian alumina refineries incur a production loss of about 20% per annum. The economic implications of this loss could be devastating to the industry if appropriate technologies are not developed to check it or at least minimise it. The presence of organics, especially those with hydroxy or electronegative groups are said to inhibit precipitation of gibbsite and/or decrease the purity of the alumina.

The understanding of how organic ligands complex with metal ions such as calcium, aluminium, gallium, lanthanum and metallate anions such as aluminate may help to improve the extractive technologies. Maximisation of metal recovery during the metal extraction process from its ore is one of the prime objectives of the metallurgical industry. Therefore it is very important to know if the presence of organic materials in the process will affect the metal being processed under the prevailing conditions, and if so, what are the mechanisms underlying the effect.

Group three elements, of which aluminium is one, form complexes readily with organic ligands containing electronegative atoms such as oxygen and nitrogen due to their smaller size and relatively large positive charge (Greenwood and Earnshaw, 1997). The availability of carboxylate, hydroxy and hydroxy carboxylate ligands, therefore, may block the nucleation sites for gibbsite crystal growth and/or complex aluminate which results in loss of alumina production (Power, 1991).

### 1.1.1 Effect of organic compounds on gibbsite precipitation

The organic carbon content of the Bayer liquors consists of compounds ranging in molecular weight from 50 to 10,000 (Lever, 1978). Lever categorised the complex mixture of Bayer organics into three groups based on the level of degradation. He classed them as high molecular weight, such as humic and fulvic acids, building block compounds, such as butyric acid, diethylene glycol, 2-hydroxy benzoic acid and low molecular weight compounds, such as oxalic, formic and acetic acids.

Smith, Watling and Crew, (1996) have studied the effects of model organic compounds on gibbsite crystallisation by deliberate dosage of acyclic polyols in supersaturated liquor. Comparison of C2-C6 alditols (figure 1) showed that, in broad terms, crystallisation inhibition strength, in terms of growth rate, increased with carbon chain length such that D-mannitol had the greatest effect and ethylene glycol the least. They concluded that as the chain gets longer, considerable flexibility is achieved which then allows optimum conformational changes for complexation and/or surface binding.

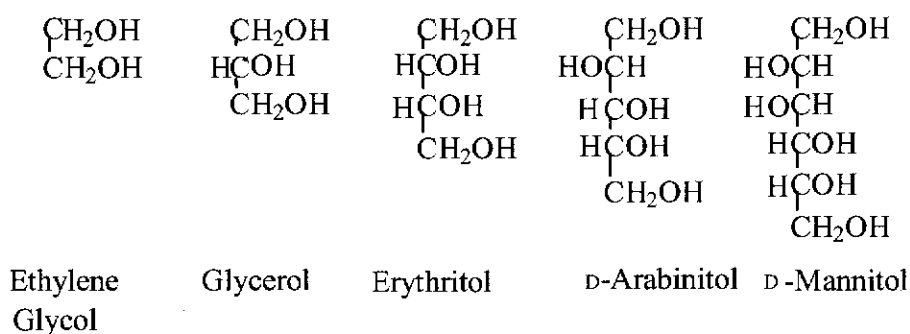


**Figure 1:** Some C2 - C6 alditols

Comparison of the effect of C5 alditol stereoisomers (figure 2) showed that the stereochemistry of the molecule with respect to the increased hydroxy groups played a vital role in the influence of gibbsite growth inhibition. Again it is likely that the alditols form zig-zag conformations (figure 3). These conformations are believed to have effected axial-equatorial-axial arrangement of hydroxy groups which favours coordination (Smith, Watling and Crew, 1996).

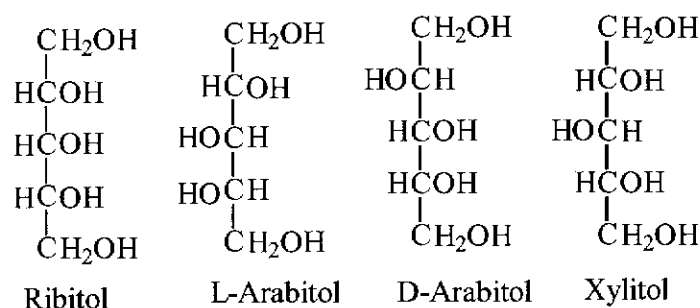


**Figure 2: C-5 Alditols**

Table 2 shows the extent of growth inhibition on gibbsite by the alditols as determined by Smith, Watling and Crew (1996) along with their electrophoretic mobilities with calcium ions in aqueous solution as determined by Angyal, Greeves and Mills (1974).

**Table 2: Gibbsite inhibition by polyols and their relative electrophoretic mobility**

Alditol	Gibbsite inhibition (%)	Mobility ( $m_i$ )
<i>cis</i> -Inositol	-	1.00
Sorbitol (C-6)	94	0.20
Xylitol (C-5)	89	0.18
Mannitol (C-6)	56	0.14
D,L-Arabinitol (C-5)	42	0.13
Ribitol (C-5)	15	0.08
Erythritol (C-4)	8	0.08

Angyal, Greeves and Mills (1974) reported that in acyclic polyols, a geometrical zig-zag conformation (an MP arrangement) of hydroxy groups (figure 3) favours coordination, as was observed with calcium ions in aqueous solution. In their work Angyal, Greeves and Mills stated that the *threo-threo* arrangement in the MP

conformation of alditols relieves a *gauche* interaction in the carbon chain such that the molecule becomes energetically more stable. A *threo* pair adjacent to a primary hydroxy group in alditols requires only rotation of the terminal C-C bond to bring the primary hydroxy group into an MP arrangement. However, conversion of an *erythro-erythro* sequence in an alditol molecule into an MP arrangement provides a less energetically favoured conformation. This argument seems to be the determining factor for the behaviour of an alditol on gibbsite crystallisation inhibition as observed by Smith, Watling and Crew (1996).

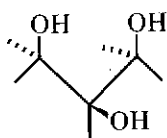


**Figure 3: An MP arrangement of hydroxy groups**

The gibbsite precipitation inhibition results parallel their complexation behaviour, for example, xylitol (C5) has a greater effect than D-mannitol despite having fewer hydroxy groups and a shorter carbon chain than mannitol (C6) (Table 2). Smith, Watling and Crew, (1996), arranged the alditols in the order of increasing inhibition of gibbsite crystallisation under Bayer process conditions as glycol < propane-1,2-diol < propane-1,3-diol < glycerol < erythritol < ribitol < arabinitol < mannitol < xylitol < sorbitol. These findings confirm the fact that presence of hydroxy organic compounds in the Bayer process results in inhibition of gibbsite crystallisation, as noted by Power (1991). However, this study did not indicate whether the inhibition was due to alditol-aluminate complexation or an adsorption onto the gibbsite or both. It is likely that alditol-aluminate complexation would reduce nucleation whereas adsorption to gibbsite would block growth sites. Despite the fact that the study indicates an involvement of an MP arrangement of alditols, it does not *a priori* suggest possible coordination sites of the flexible alditols. A study of rigid polyols such as the inositols would more readily indicate the possible hydroxy groups involved in the complexation. Generally, the complexation of metals by polyols is very complex and not well understood. However it would appear that in acyclic alditols the *threo - threo* arrangement is favoured because the molecules become

energetically stable. According to Angyal, Greeves and Mills, (1974), acyclic alditols take up an extended planar *zig-zag* conformation in solution provided that the molecule has no oxygen atoms with parallel 1,3- interactions. Complexation favours a parallel 1,3 - interaction which will be more favourable if the alditol can adopt an extended *zig - zag* rather than a bent or sickle form. This is the case for a *threo - threo* conformation, but *erythro - threo* and *erythro - erythro* conformations produce bent and sickle arrangements respectively upon complexation.

## 1.2 CYCLITOLS

Cyclitols (cyclic polyols) are a group of relatively rigid compounds which display varying characteristics with respect to cation-ligand coordination. The most commonly studied cyclitols are the inositols or cyclohexanehexols, (Guthrie and Honeyman, 1968; Painter, 1996) the diastereoisomers of which are shown in figure 4.

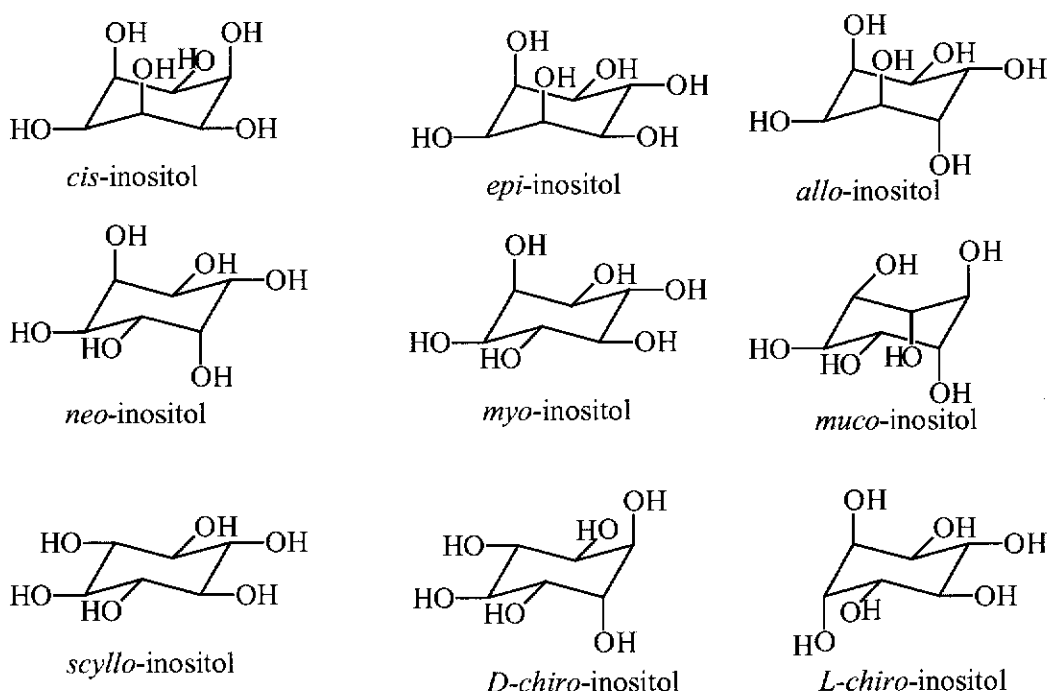


**Figure 4:** Diastereoisomers of inositol (Painter, 1996)

All nine isomers are known and all but the *chiro* isomers are meso and are therefore optically inactive compounds. *myo*-Inositol occurs widely in nature and also as phosphate esters. *scyllo*-Inositol is usually found in plants as the monomethyl ether, as are the *chiro*-inositols (Guthrie and Honeyman, 1968). The other inositols do not occur naturally and are prepared by chemical methods. The most common method of preparation is the catalytic hydrogen reduction of hexahydroxybenzene or tetrahydroxybenzoquinone followed by chromatographic separation of the individual inositols.

### 1.2.1 Synthesis of cyclitols

#### 1.2.1.1 Permanganate hydroxylation of 1,3-cyclohexadiene

The fact that cyclitols have differences in coordination is one of the determining forces for the development of stereospecific synthetic procedures. One of these (Akbulut and Balci, 1988) involves the direct hydroxylation of 1,3-cyclohexadiene using permanganate to give a mixture of 1,2,3,4-cyclohexanetetrols (figure 5).

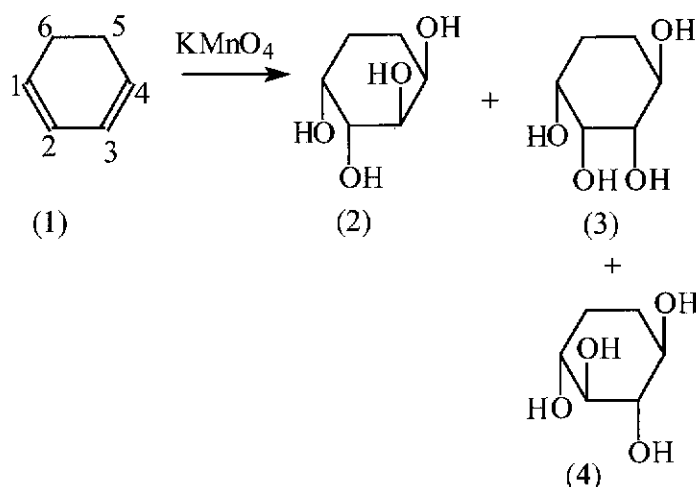


**Figure 5:** Permanganate hydroxylation of 1,3 cyclohexanediene

The results of this hydroxylation showed that it is possible to hydroxylate 1,3-cyclohexadiene to give cyclitols with four hydroxy groups. However, a significant disadvantage of this procedure is that the hydroxylation resulted in a mixture of cyclitols which required further separation into individual compounds.

### 1.2.1.2 Diels-Alder synthesis of cyclitols

ApSimon (1973) presented a comprehensive review of the synthetic chemistry of cyclitols with reference to Diels-Alder reactions (figure 6). He further reported that the synthesis of cyclitols, as described below, could not yield *cis*-inositol because the opening of the 1,4-oxobridge of compound 7, shown in figure 6 as the exoisomer, would always give *trans*-products. In his presentation it is mentioned that the reaction involved furan (5) and vinylene carbonate (6) to yield exo1,4-anhydro-*cis*-conduritol carbonate (7). Consequently the 1,4-anhydro-*cis*-conduritol carbonate is then subjected to various conditions (figure 6) to yield *epi*-inositol (8), *neo*-inositol (9), cyclohexanetetrol (10) and conduritol-c (11). The problem with this method is that permanganate hydroxylation would always yield mixed products (figures 5 and 6).

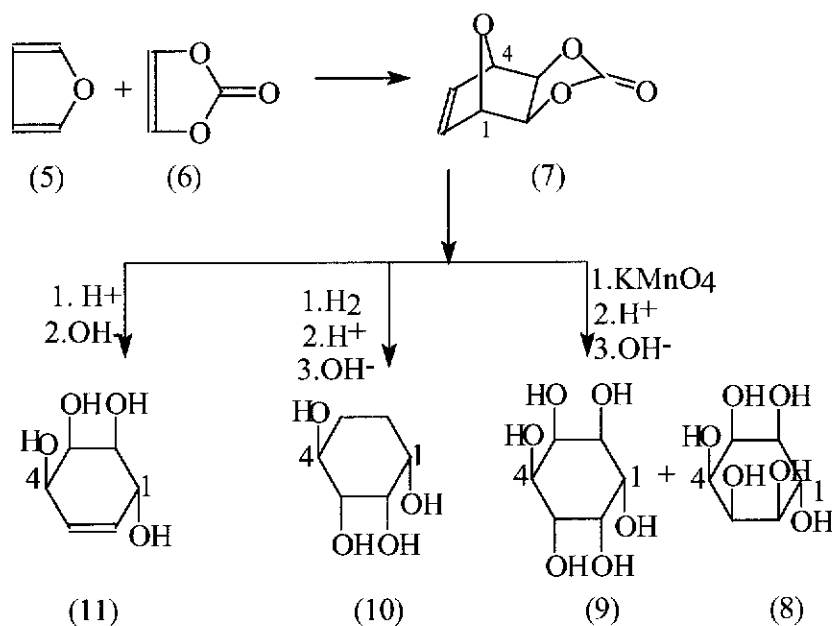


Figure 6: Diels-Alder synthesis of cyclitols.

### 1.2.2 Synthesis of *cis*-inositol

#### 1.2.2.1 Synthesis from *epi*-inositol

Angyal and Hickman (1971) reported that *cis*-inositol could be synthesised from *epi*-inositol in seven steps with an overall yield of 25% (figure 7). This method provided a practical synthesis of *cis*-inositol at that time. The problem is that the method is

long and the yield is low. Another problem is that it requires *epi*-inositol as starting material which is prepared from *myo*-inositol in low yields (10%) (Posternak, 1952).

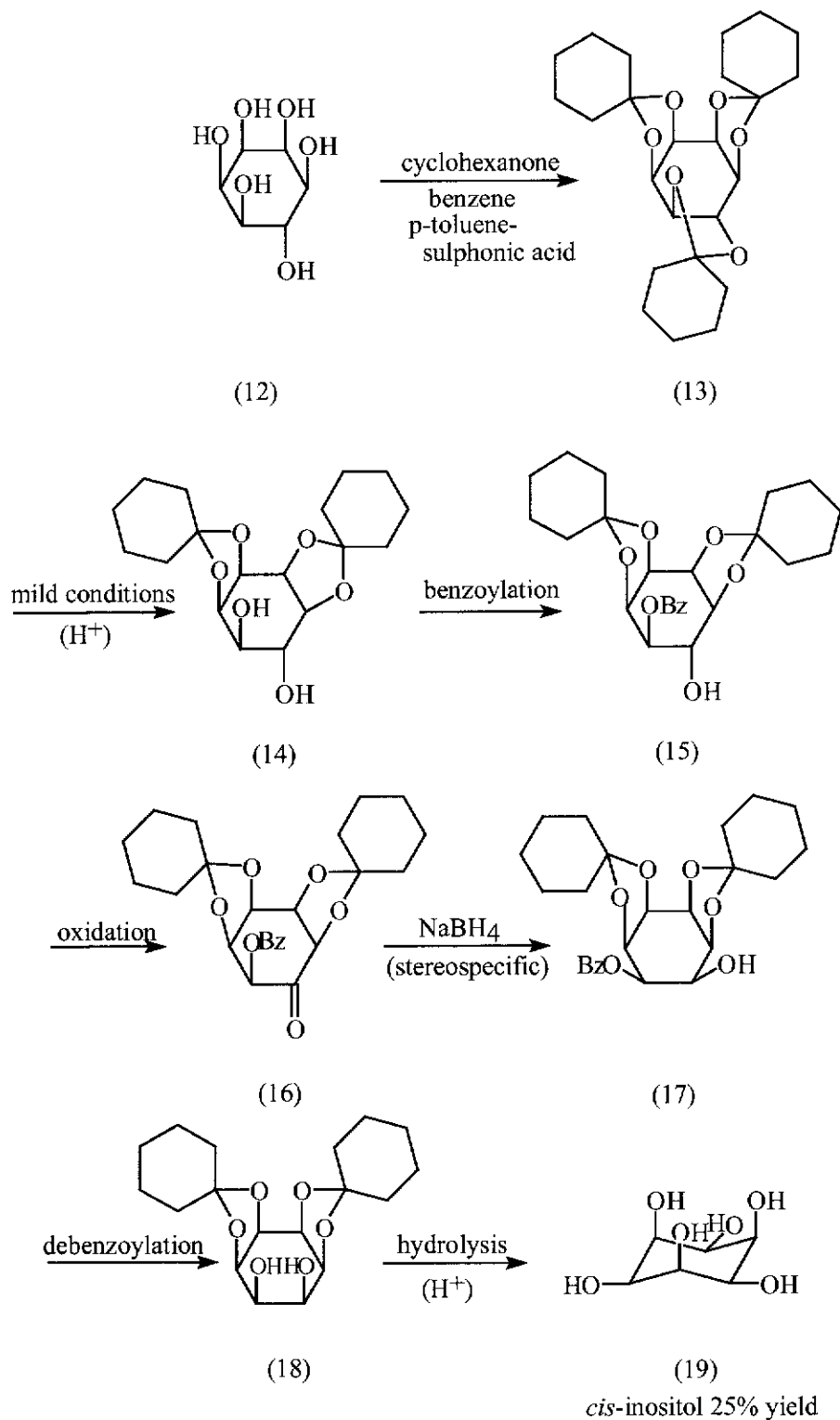


**Figure 7:** Synthesis of *cis*-inositol from *epi*-inositol (Angyal and Hickman, 1971)

### 1.2.2.2 A simple synthesis of *cis*-inositol

It was not until 1995 that Angyal, Odier and Tate developed a one step synthesis of *cis*-inositol by the catalytic hydrogenation of tetrahydroxyquinone (figure 8).

However, the purification stage of this method is a deterrent factor as the chromatographic separation is a slow process and it is necessary to evaporate large volumes of water to recover the *cis*-inositol in moderate yields (~30%).

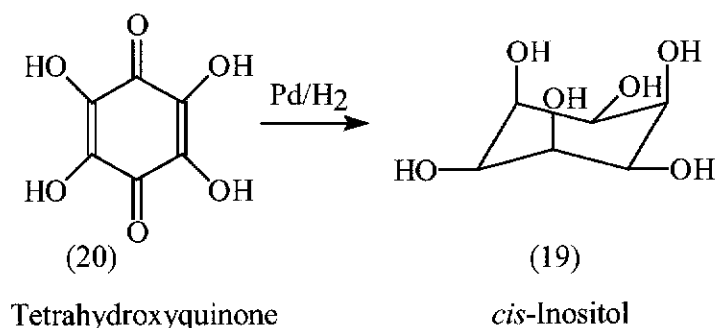


Figure 8: Catalytic reduction of tetrahydroxyquinone to *cis*-inositol

Although the isolation and purification of *cis*-inositol by the hydrogenation method is long and tedious, it was judged to be superior to the multistep process. In the multistep process *epi*-inositol is converted to *cis*-inositol in 25% yield, but *epi*-inositol must be prepared from *myo*-inositol and this is achieved in only 20% yield. Accordingly the overall yield from *myo*-inositol is about 5% which is much lower than in the catalytic reduction of tetrahydroxyquinone. The multistep method therefore requires more material input and is therefore relatively expensive. Consequently, synthesis of *cis*-inositol in this work was carried out according to Angyal, Odier and Tate (1995) because the method was judged to be more efficient.

### 1.2.3 Synthesis of *epi*-inositol

Unlike *cis*-inositol (19), *epi*-inositol (23) is readily synthesised and purified, although the yield is low. The critical stage in this method is the purification of (22) through *epi*-inosose-2-phenylhydrazone. Based on the principle of hydrazine condensation of carbonyl groups, the *epi*-inosose is effectively reacted to give the crystalline orange

*epi*-inosose-2 phenylhydrazone which is easily purified. Hydrolysis of the hydrozone gives pure *epi*-inosose (22) which is reduced to *epi*-inositol (23). This synthesis of *epi*-inositol as reported by Posternak, (1952), is based on the oxidation of *myo*-inositol (21) with concentrated nitric acid to form an intermediate product, *epi*-inosose (22) which usually is mixed with unreacted *myo*-inositol. In order to obtain the pure *epi*-inositol, the intermediate product, *epi*-inosose is selectively removed from the mixture through the phenylhydrazone purification (figure 18).

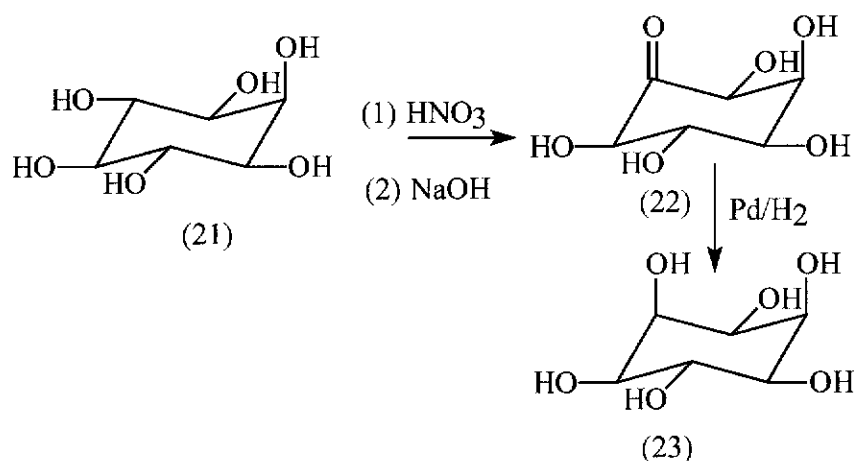


**Figure 9:** Synthesis of *epi*-inositol (Posternak, 1952)

### 1.3 COORDINATION ABILITIES OF THE INOSITOLS

Angyal and Hickman (1975) reported that of the nine diastereoisomers of inositols, *cis*-inositol has the strongest complexing ability with  $\text{Ca}^{2+}$ ,  $\text{Sr}^{2+}$  and  $\text{Ba}^{2+}$  as shown by their electrophoretic mobility. It has been reported that the strong complexing ability of *cis*-inositol arises because the molecule has a *syn-axial* arrangement of hydroxy groups. Although the complexing abilities of the inositols were recognised as early as 1825 (Angyal, 1989), serious scientific papers discussing in more detail inositol-cation relationships emerged only as recently as 1971, when Angyal and Hickman studied complex formation between sugars and metal ions.

Many studies undertaken to investigate metal coordination chemistry with these compounds have shown that triaxial and sequential axial-equatorial-axial arrangements of hydroxy groups (figure 10) favour coordination (Angyal, 1989).

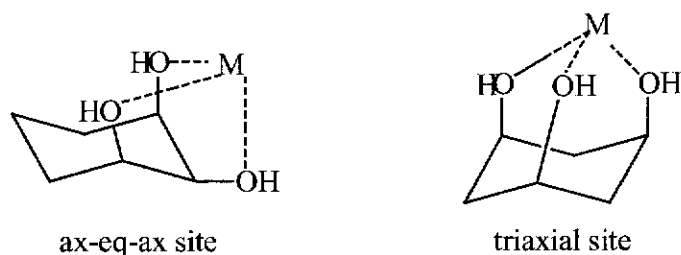


**Figure 10:** Ax-eq-ax and triaxial coordination sites

Angyal and Hickman (1971) reported that because *cis*-inositol (figure 8) has all its six hydroxy groups in a *cis* arrangement to each other and that each of its equivalent chair conformers has three *syn-axial* hydroxy groups, it forms strong complexes with borate anions and many cations. These early studies revealed interesting chemical properties of inositols and prompted carbohydrate chemists to intensify studies on cyclitol-cation complexation. The ionic size of a cation has been observed as a vital factor in determining the configuration of a complex (Angyal, 1989; Dill and Carter, 1989). They found that metal ions having radii of about 100 pm readily coordinate at the ax-eq-ax site of *cis*-inositol and *epi*-inositol whereas metal ions with radii less than 80 pm will fit in the triaxial cavity.

A number of methods have been used for the detection of coordination and structure, such as nuclear magnetic resonance spectroscopy (NMR, both proton and carbon), electrophoresis, infrared spectroscopy (IR), high performance liquid chromatography (HPLC), x-ray crystallography and thin layer ion exchange chromatography (TLIEC) (Angyal, 1989; Dill and Carter, 1989).

### 1.3.1 Infrared spectroscopy

Although infrared spectroscopy (IR) has been used to study complexation, the results of most studies provided little or no specific information in respect of complexation modalities and structure. However, a critical study was conducted by Tajmir-Riahi (1983) when he studied IR spectra of crystalline D-Glucuronic acid and its calcium complexes in the region 4000-400  $\text{cm}^{-1}$ . It was observed that the absorption bands arising from the intramolecular hydrogen bonding of the free sugar molecules shifted to lower frequencies by about 25  $\text{cm}^{-1}$  when complexed, whereas an absorption band

at  $3160\text{ cm}^{-1}$  disappeared upon ionisation of the acid. He suggested that this result indicated that the complexation of the free sugar breaks the intramolecular hydrogen bonding system whereas the strong intermolecular hydrogen bonding network is retained. A point worthy of noting in this work is that there were many IR peaks which may have led to inaccuracies in assignment of specific bonds to particular IR bands. This method is therefore best applied to simple molecules with a simple IR spectrum.

### **1.3.2 High performance liquid chromatography**

High performance liquid chromatography (HPLC) and gas liquid chromatography (GC) have been used to separate organometallic complexes. Veening and Willeford (1979) reported that metal coordination complexes have been successfully separated by application of liquid-liquid partition HPLC, ion exchange HPLC and size exclusion HPLC. In assessing these methods, they pointed out that reverse phase HPLC was by far the most popular and promising method for separation of a variety of organic complexes and biologically active compounds. They reported that very little had been done in this area, and that the only notable work was the application of reverse phase HPLC to separate neutral tetradentate chelates of copper(II), nickel(II) and palladium(II) with fluorinated and non-fluorinated  $\beta$ -ketoamine and salicylaldimine ligands. In their review Veening and Willeford (1979) reported that the separation of the complexes was achieved by using a bonded octadecyl substrate as a reverse phase functionality under isocratic elution with water, methanol and acetonitrile with UV detection at 254nm. A very clear limiting factor in this method is the fact that it is exclusive to ligands with chromophores in the ultraviolet or visible region.

### 1.3.3 NMR coordination studies

Extensive work in the area of polyol-metal coordination by NMR spectroscopy has been published. Symons, Benbow and Pelmore (1984) found that changes in NMR chemical shifts which occur due to complex formation give a guide to the structure of the resultant complex. These observations enabled possible complexing sites of the ligand to be determined. Similarly, Angyal (1989) observed that complex formation between a ligand and a cation caused chemical shift changes in the NMR spectra of polyols and carbohydrates. He further indicated that establishment of the equilibrium between polyols and cations in aqueous solutions is fast on the NMR time-scale. This observation applies to polyols without bulky side chains or groups which may pose steric hindrance, a factor which became evident when Angyal, Greeves and Littlemore (1985) studied the coordination behaviour of muellitol (24).

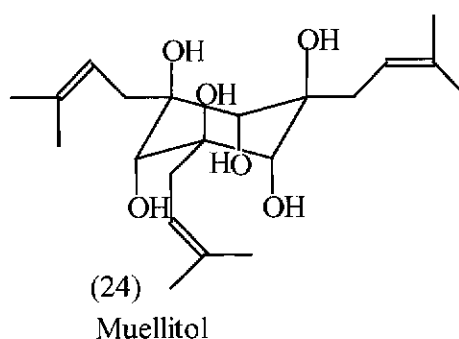
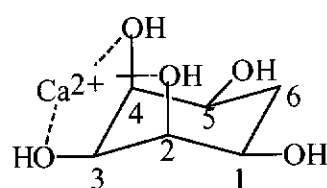
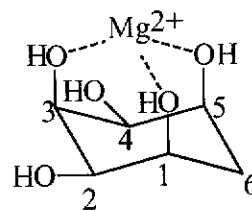


Figure 11: Structure of muellitol

They found that muellitol (24) displayed slow exchange between the complex and its components, most likely due to the presence of bulky side chains in the molecule. This implies that the bulky side chains of muellitol (24) pose steric hinderance to the complexation process, in which case, the establishment of the equilibrium between muellitol (24) and its cation complex in aqueous solution is slow on the NMR time-scale. Angyal (1989) observed that in the  $^1\text{H}$  NMR spectrum of cyclohexane 1,2,3,4,5/0-pentol (figure 12), on addition of calcium ions (99 pm), the signal of H-3 shifted strongly downfield.



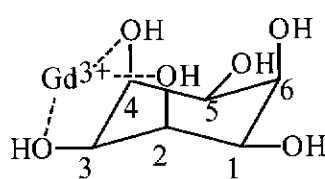
(25)



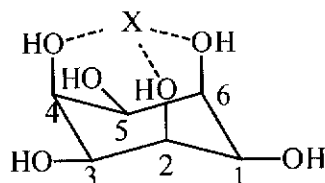
(26)

**Figure 12: Possible complexation of 1,2,3,4,5/0-cyclohexane-pentol conformation**

This phenomenon was interpreted as an indication that complexation occurred at O-2, O-3 and O-4 because H-3 is on the central carbon at the vicinal tridentate binding site. When magnesium ions were added a different pattern of results was observed. Angyal (1989) indicated that addition of magnesium ions to cyclohexane 1,2,3,4,5/0-pentol showed significant induced downfield chemical shift changes on H-1, H-3 and H-5. Accordingly, it was suggested that ring inversion occurred such that  $Mg^{2+}$  ions (72pm) coordinated in the triaxial site (figure 12 (26)). This observation showed that the size of a cation plays a vital role in coordination chemistry. To further demonstrate this, Dill and Carter (1989) compared the effect of  $Gd^{3+}$  (94 pm) and  $Mg^{2+}$  (72 pm) on the  $^{13}C$  NMR spectra of *epi*-inositol and  $Cu^{2+}$  (73 pm) and  $Mn^{2+}$  (80 pm) on *cis*-inositol (figure 13). The results showed that  $Gd^{3+}$  has substantial effect on the signals of C-2, C-3 and C-4 whereas  $Mg^{2+}$  did not. On the other hand, addition of  $Mn^{2+}$  and  $Cu^{2+}$  ions to *cis*-inositol solutions broadened signals of carbon atoms bearing axial hydroxy groups more than the equatorial ones. Dill and Carter (1989) suggested that the trends of coordination are as shown below.



(27)



(28)  $X = Cu^{2+}$  or  $Mn^{2+}$

**Figure 13: Coordination sites of *cis*-inositol**

Based on this argument, they concluded that the smaller ions are better coordinated in the triaxial cavity than in the ax-eq-ax hole and *vice versa* for large cations and

that ionic charge had little or no effect on the coordination site. This argument seems logical, however, while size of the cation is a vital factor, it cannot be said conclusively that  $\text{Mn}^{2+}$  and  $\text{Cu}^{2+}$  coordinated to O-2, O-4 and O-6 of *cis*-inositol. The reason being that *cis*-inositol has four coordination sites, three ax-eq-ax and one triaxial. Thus from a close look at the figure 13 (27) one may suggest a possibility of coordination at O-4, O-5, and O-6. At this position, two axial hydroxy groups (O-4 and O-6) are involved and thus a more significant effect on their signal will be observed than on the others. In this respect, the results can only be confirmed if a molecule of the conformation as shown in figure 14, was used because it would be certain that complexation only occurred at a triaxial cavity since inversion is not possible nor are alternative coordination sites available.

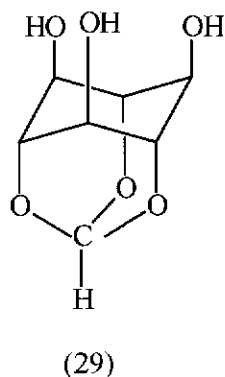


**Figure 14: Scyllo-inositol orthoformate: triaxial site- only site for coordination**

Similar work and observations were made by Angyal, Greeves and Pickles (1974) when they reported that the signal of the methyl hydrogen in the  $^1\text{H}$  NMR spectrum of 2-deoxy-2-methyl-*epi*-inositol (30), shifted upfield on addition of either calcium or magnesium ions suggesting a possibility of ring inversion to provide a favourable coordination site (31).

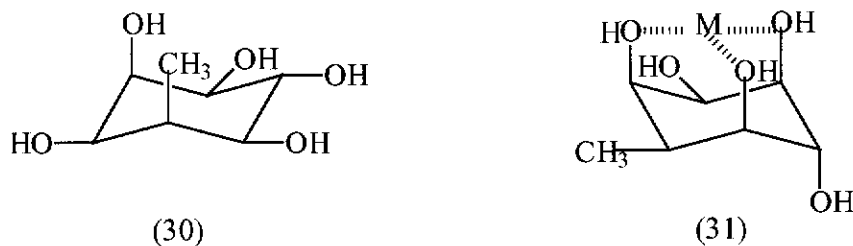


**Figure 15: Ring inversion of 2-deoxy-2 methyl *epi*-inositol**

Angyal, Littlemore and Gorin (1985) studied  $^{13}\text{C}$  NMR chemical shift changes of *epi*-inositol induced by various lanthanide ions in deuterated water ( $\text{D}_2\text{O}$ ). From the chemical shift data, they deduced that lanthanide cations such as  $\text{La}^{3+}$ ,  $\text{Ce}^{3+}$ ,  $\text{Pr}^{3+}$ ,  $\text{Nd}^{3+}$ ,  $\text{Sm}^{3+}$ ,  $\text{Eu}^{3+}$  and  $\text{Tb}^{3+}$  cause changes in the  $^{13}\text{C}$  NMR spectra of *epi*-inositol which showed no regularity. They suggested that the reason for this is that ionic radii decrease along the lanthanide series which on coordination, affected bond angle distortions differently.

NMR spectroscopy can also be used to obtain formation constants of metal-organic complexes. Beatie and Kelso (1981) used  $^{13}\text{C}$  NMR data to estimate the equilibrium constant of calcium-sorbitol (*D*-glucitol) complexes in  $\text{D}_2\text{O}$ . They assumed that the chemical shifts reflected an equilibrium between uncomplexed sorbitol and a single calcium-sorbitol complex. Hence, they were able to deduce equilibrium dynamics of the complex and uncomplexed ligand but did not propose a structure for the complex. Based on this assumption they formulated a relationship between the equilibrium constant and the chemical shift of each resonance as follows:

$$1/d_{\text{obs}} = 1/d_c + 1/(d_c K[\text{Ca}^{2+}]).$$

Where :  $d_c$  is the difference in chemical shifts of uncomplexed and complexed  
 $d_{\text{obs}}$  is the shift from the resonance position of uncomplexed ligand  
 $K$  is the equilibrium constant.

In this work, Beatie and Kelso determined an equilibrium constant of calcium-sorbitol complexation system for each carbon atom by plotting  $1/d_{\text{obs}}$  against  $1/[\text{Ca}^{2+}]$  (Table 3).

**Table 3: Equilibrium constants,  $K$ , of *D*-glucitol calcium complex derived from  $^{13}\text{C}$  NMR chemical shifts (Batie and Kelso 1981)**

Carbon atom	$K (\text{Lmol}^{-1})$ 4°C	$K (\text{Lmol}^{-1})$ 36°C
C1	$1.9 \pm 0.7$	$0.7 \pm 0.7$
C3	$0.7 \pm 0.2$	$0.2 \pm 0.2$
C4	$1.6 \pm 0.4$	$1.1 \pm 0.4$
C6	$0.5 \pm 0.4$	$0.2 \pm 0.4$

Similar work was undertaken by Angyal and Hickman (1975) when they studied complexes of carbohydrates with metal cations. In their work they reported that if a divalent cation ( $M^{2+}$ ) and ligand (L) combine reversibly to form a 1:1 complex ( $ML^{2+}$ ) then, K, the stability constant can be determined by:

$$K = ([ML^{2+}]/[M^{2+}][L])(A_{ml}/A_m A_l).$$

Where:  $A_{ml}$  is activity coefficient of complex  
 $A_m$  is activity coefficient of metal cation  
 $A_l$  is activity coefficient of ligand

If the activity coefficients are known and concentrations of the complexed and uncomplexed species are also known, then the value of K can be calculated.

However, Angyal and Hickman (1975) noted that the above assumption did not work well with *cis*-inositol because *cis*-inositol tended to form 1:2 complexes in which case two constants needed to be defined. Using an ion-selective electrode to measure cation concentrations, they found the stability constants of *epi*-inositol with calcium, strontium and barium were 2.2, 2.1 and 1.8 Lmol<sup>-1</sup> respectively. However, using the same method for *cis*-inositol, it was found that the calculated constants varied between 10 to 20 Lmol<sup>-1</sup> suggesting the possibility of 1:2 ligand:cation complex. Angyal (1989) reported that this stoichiometry phenomenon coupled with non-availability of standard values of activity coefficients of ions led to unsatisfactory determination of stability constants of cation-ligand complexes. However, approximate complex stability constants have been calculated using known concentrations and the assumption that coordination is 1:1. The stability constant values determined in this way provide a guide on how strongly or weakly a particular ligand coordinates with different cations.

Application of NMR spectroscopy in coordination studies provides vital information regarding the configuration of the ligand-cation complex and also approximate complex formation constants can be calculated.

### 1.3.4 Paper electrophoresis

An early popular method for coordination studies was paper electrophoresis. Angyal and Mills (1979) reported that paper electrophoresis in an electrolyte containing calcium ions is a suitable method for the separation and characterisation of many polyols. Although this method is also useful for detection of complex formation between a ligand and a cation in solution, it does not provide structural or stoichiometric information for the resultant complex. Relative electrophoretic mobility values will show the extent of coordination and can be used to approximate complexing abilities of various ligands. However, geometry and size of the resultant complex plays a vital role to influence the level of mobility of the complex in an electrolyte (Angyal and Mills 1979). Angyal and Mills (1979 and 1985) observed that cyclitol complexes migrate towards the cathode and that the rate of mobility indicates the relative extent of coordination. Electrophoretic mobilities of some cyclitols such as *cis*-inositol, *epi*-inositol and other polyols that have *axial-equatorial-axial* hydroxy group arrangement are easily detected (Angyal, 1989). Among the cyclitols however, *cis*-inositol has been observed to have the greatest mobility with all the cations studied, hence, *cis*-inositol has been used as a reference material in many complexation studies (Angyal, 1989 and Angyal and Mills, 1985) (Table 4).

**Table 4: Relative electrophoretic mobilities of some cyclitols.**

Inositol	Mobility ( $M_i$ )
<i>cis</i> -inositol	1.0
<i>epi</i> -inositol	0.44
<i>allo</i> -inositol	0.48
<i>muco</i> -inositol	0.11
<i>myo</i> -inositol	0.07
<i>scyllo</i> -inositol	0.04

Although electrophoretic mobility gives a quick indication of coordination ability of cyclitols, it does not provide information of resultant complex structure nor can the data be used to approximate stability constants. Comparatively therefore, NMR spectroscopy is a much better method than electrophoresis.

### 1.3.5 Ion exchange thin layer chromatography

In this method, complexation abilities of polyols is ascertained by comparing  $R_f$  values on an ion exchange thin layer plate. Angyal (1989) reported that compounds which complex strongly are retained and have low  $R_f$  values whilst those that complex weakly move with the solvent front, having  $R_f$  values  $\sim 0.9$ . Complex formation and how strongly a ligand forms complexes with a particular cation can thus be detected easily by this method and a qualitative description and comparison can also be achieved. Again, the problem with this method is that no information regarding the structure of the resultant complex is provided. Angyal and Craig (1993) applied ion exchange chromatography to determine  $R_f$  values of several carbohydrates, both cyclic and acyclic (Table 5).

**Table 5: Ion exchange  $R_f$  values (Angyal and Craig, 1993)**

Polyol	$\text{La}^{3+}$	$\text{Ce}^{3+}$	$\text{Pr}^{3+}$	$\text{Nd}^{3+}$	$\text{Sm}^{3+}$
Xylitol	0.48	0.46	-	0.39	0.33
Ribitol	0.75	-	-	0.70	-
Arabinitol	0.65	0.60	-	0.54	-
Altritol	0.66	0.58	-	0.50	-
Fructose	0.71	0.73	0.74	0.74	-
<i>epi</i> -inositol	0.39	0.34	-	0.28	0.15

Clearly, these data show that cations coordinate to a different extent with each of the ligands, but that the relative ability of the carbohydrate to form complexes does not change significantly. For example,  $\text{La}^{3+}$ ,  $\text{Ce}^{3+}$  and  $\text{Nd}^{3+}$  show that the coordination trend is *epi*-inositol > xylitol > arabinitol  $\sim$  altritol > fructose  $\sim$  ribitol.

This method is useful in that like electrophoretic mobility, a quick guide of complexation trends of the carbohydrates can be obtained. However, stability constants of complexes cannot be determined, and neither can structural information for the complexes, so therefore NMR spectroscopy is also superior to this method.

### 1.3.6 X-ray crystallography

One of the most powerful methods in ligand-cation complex structure determination is X-ray crystallography. Angyal and Craig (1993) used X-ray crystallography to determine the crystal structure of galactitol. $2\text{PrCl}_3 \cdot 14\text{H}_2\text{O}$  and hence determined the oxygens which were involved in coordination. They observed that the cation was coordinated to ligand oxygen atoms in addition to water molecules and that hydrogen bonding reinforced the structure. Clearly this work provides vital information on how cation-hydroxy group coordination occurs although the crystalline structure may not necessarily provide evidence for the structure of the complex in solution. Burger and Nagy (1990) pointed out that when such crystalline complexes are dissolved in water, the hydrogen bonds may break and the solvent molecules, usually water, will replace the ligand from the coordination. In which case, only strongly bound complexes will persist. Dheu-Andries and Perez (1983) reviewed in more detail the structures of sugar complexes with calcium cations. They observed that, generally, calcium ions are coordinated to eight oxygen atoms in a square-antiprismatic arrangement. An example of this type of coordination is that provided by Ollis *et al.* (1978) as shown in figure 16 where ax-eq-ax oxygens are involved.

It should be pointed out that complexation studies by x-ray method is only useful if the resultant complexes are sufficiently stable such that they can be isolated and single crystals grown for x-ray analysis.

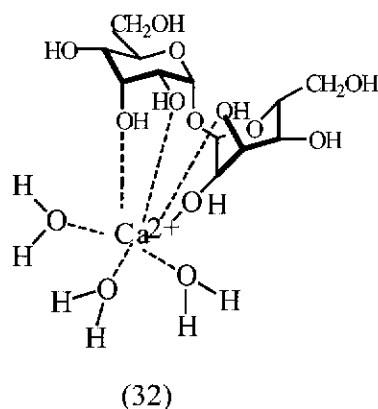


**Figure 16: Calcium complex of D-allopyranosyl-D allopyranoside**

## 1.4 SCOPE OF THIS PROJECT

This project aimed to study the interaction of cyclic polyols (inositols) with metal cations and metallate anions to gain an understanding of the likely behaviour of organic compounds in Bayer liquors. The results may help identify potential crystallisation poisons and add to the understanding of inhibition in gibbsite precipitation. This aim was to be met by the following objectives:

### 1.4.1 Synthesis of inositols

Synthesis of ligands as only *myo*-inositol was readily available. *cis*-Inositol and *epi*-inositol are either unavailable commercially or prohibitively expensive.

### 1.4.2 Coordination modalities

The coordination modalities of  $\text{Al}^{3+}$  with some inositols, in comparison with other cations such as  $\text{Ca}^{2+}$ ,  $\text{Ga}^{3+}$ ,  $\text{La}^{3+}$  and  $\text{Sm}^{3+}$ , under neutral conditions, using,  $^{13}\text{C}$  NMR, HPLC and ion exchange thin layer chromatography were investigated. The basic objective was to compare the coordination abilities of the cations and inositols and determine possible coordination sites of the ligands and the effects of configuration and cation size, and hence, possible structures of the complexes formed.

### 1.4.3 Coordination trends under basic conditions

Coordination studies with aluminate are an important aspect in relation to the Bayer Process, which operates under basic conditions.  $^{13}\text{C}$  NMR spectroscopy experiments of inositols /aluminate interactions, when compared with cation data, would be expected to give information with respect to ligand coordination sites and possibly the nature of the aluminate-inositol interaction.

## CHAPTER 2- Experimental Procedures

### 2.1 GENERAL EXPERIMENTAL DETAILS

#### 2.1.1 Nuclear magnetic resonance (NMR) spectra

NMR spectra were obtained by using a Varian Gemini 200MHz NMR spectrometer.  $^{13}\text{C}$  NMR spectra were recorded at a frequency of 50MHz. Two solvent systems were used, deuterated water ( $\text{D}_2\text{O}$ ) with *tertiary*-butyl alcohol as an internal standard at a chemical shift of 31.6ppm and deuterated chloroform ( $\text{CDCl}_3$ ) with a solvent reference chemical shift of 77.7ppm. For better resolution and heteronuclear correlation (HETCOR) data, a Bruker 500MHz instrument was used. Errors were based on the digital resolution set for the acquisition of spectra (0.3 Hz/pt). Therefore an error of +/- 0.6 Hz (approximately 0.01 ppm) was assumed in this work.

#### 2.1.2 Infrared (IR) spectra

Infrared spectra were acquired using a Bruker Vector 22 Fourier Transform Infrared spectrometer (4000-400  $\text{cm}^{-1}$ , 4  $\text{cm}^{-1}$  resolution, using the KBr disc technique) and a Bruker IFS 66 (4000-400  $\text{cm}^{-1}$ , 4  $\text{cm}^{-1}$  resolution) for horizontal attenuated total reflectance measurements of solutions.

#### 2.1.3 High performance liquid chromatography (HPLC)

A Waters 410 HPLC was used for all HPLC analyses with the following conditions:

Pressure : 2500 psi

Detector : Waters differential refractometer

Column : 5 *micron*, spherical  $\text{C}_{18}$  reverse phase (Supelco).

Flow rate : 0.6mL/minute

## 2.2 CHEMICALS AND MATERIALS USED

**Table 6: Chemicals and materials used**

Name	Grade	Source
glyoxal solution(40%)	AR	Aldrich Chemicals
Ethyl acetate	AR	Ajax Chemicals
Petroleum spirit	AR	Ajax Chemicals
Ethanol	GP	Ajax Chemicals
Methanol	AR	Ajax Chemicals
Aluminium sulphate	AR	BDH Chemicals
Gallium oxide	AR	Aldrich
Calcium chloride	AR	BDH Chemicals
Samarium oxide	AR	Aldrich
Lanthanum oxide	AR	Aldrich
Pyridine	AR	Ajax Chemicals
Phenylhydrazine	AR	BDH Chemicals
Sodium sulphate	AR	Ajax Chemicals
Sodium hydroxide	AR	Ajax Chemicals
Sodium sulphite	AR	Sigma Chemical Co. Inc.
<i>myo</i> -Inositol	AR	Sigma Chemical Co. Inc.
N,N-Carbonyldiimidazole	AR	Sigma Chemical Co. Inc.
Silica gel	AR	Ajax Chemicals
Dowex x2 (100-200 mesh)	AR	Aldrich Chemicals
Hydrochloric acid	AR	BDH Chemicals
Nitric acid	AR	BDH Chemical Co.

Sulphuric acid	AR	Aldrich Chemical Co.
Hydrogen gas	HP	BOC Gases
Nitrogen gas	HP	BOC Gases
Acetone	GP	Ajax Chemicals
Tertiary butylsilyl chloride	AR	Aldrich Chemicals
Chloroform	AR	Ajax Chemicals
Palladium metal	Coin (99.9%)	Perth Mint
Tertiary butyl alcohol	A.R.	BDH Chemicals
Deuterated chloroform	99%	BDH Chemicals
Sodium chloride	AR	Ajax Chemicals
Deuterated water	99%	ANSTO
Trichloroacetic acid	AR	BDH Chemicals
Trifluoroacetic acid	AR	Fluka Chemicals

## 2.3 SYNTHESSES

### 2.3.1 Tetrahydroxyquinone

Tetrahydroxyquinone was synthesised according to the procedure described by Fatiad and Sager, (1973) (figure 17), in a yield of 7.5% (literature 6.2-8.4%, m.p. 310-315 °C, literature >300 °C, Aldrich (1990-1991)).

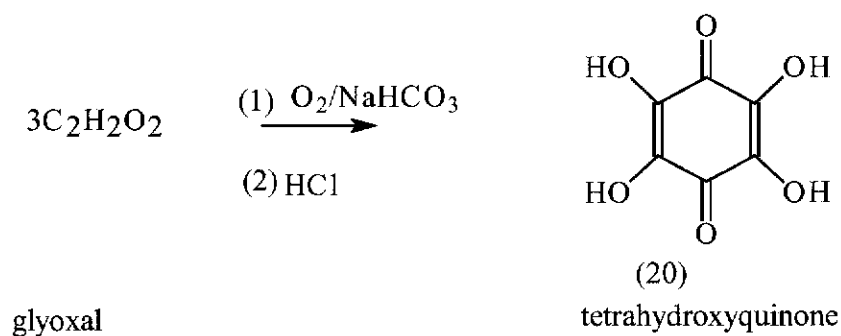


Figure 17: Synthesis of tetrahydroxyquinone

The tetrahydroxyquinone was synthesised to be used as the starting material for the synthesis of *cis*-inositol as described by Angyal, Odier and Tate (1995).

### 2.3.2 Synthesis of *epi*-inositol

Synthesis of *epi*-inositol (23) was carried out according to the method described by Posternak (1952). *Myo*-inositol (33) was oxidised by concentrated nitric acid on a hot plate in a porcelain dish and then neutralised with concentrated sodium hydroxide solution to obtain DL-*epi*-inosose (34). The DL-*epi*-inosose was treated with phenylhydrazine solution in acidic condition to yield DL-*epi*-inosose-2 phenylhydrazone (35). This step is necessary to separate DL-*epi*-inosose from the unoxidised *myo*-inositol which remained in solution. The hydrazone was then selectively oxidised under acidic and hot conditions to yield pure *epi*-inosose (34). The *epi*-Inositol was obtained in a low yield of 10%, m.p. 190-196 °C (Posternak 1952, 190-196 °C) by reduction of *epi*-inosose under a hydrogen atmosphere with palladium metal as a catalyst. The heteronuclear correlation spectra gave the following assignments: C-3, 68.8 ppm, C-6, 72.0 ppm, C-1,5, 73.8 ppm and C-2,4, 76.5 ppm. This assignment is consistent with published data by Angyal and Odier (1982), 67.8, 71.1, 72.7 and 75.5 ppm.

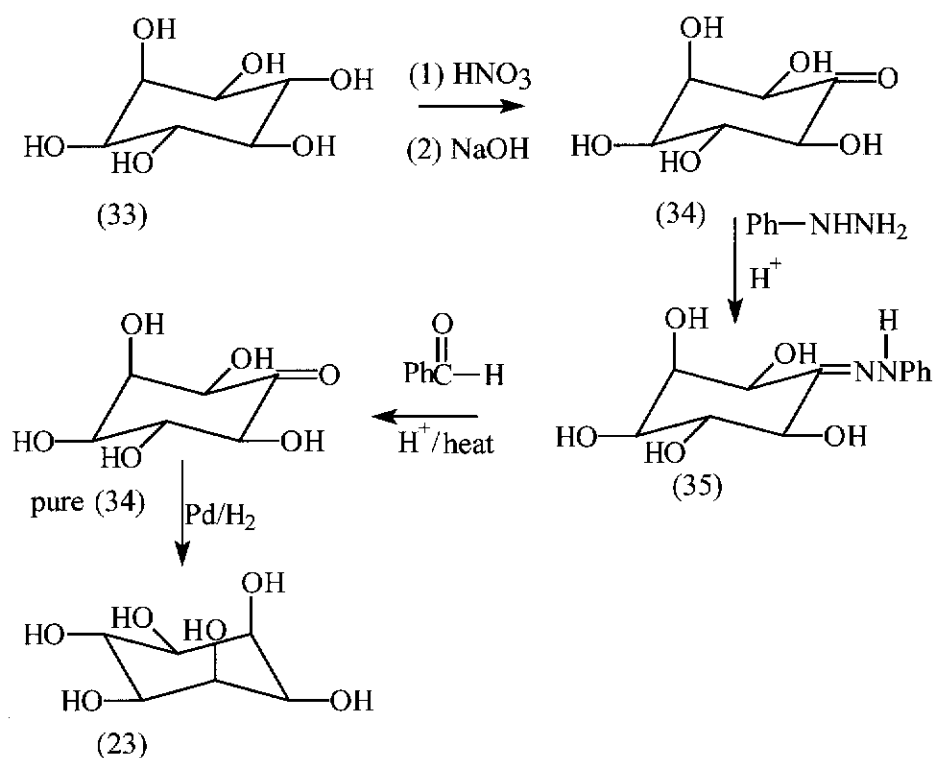


Figure 18: Synthesis of *epi*-inositol

### 2.3.3 Synthesis of *cis*-inositol from tetrahydroxyquinone

The synthesis of *cis*-inositol (19) was carried out by following the method described by Angyal, Odier and Tate (1995).

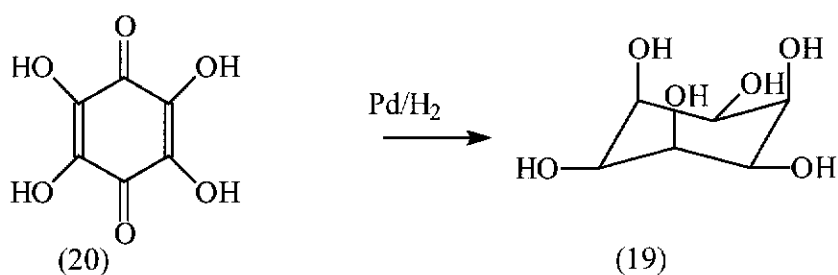


Figure 19: Synthesis of *cis*-inositol

Tetrahydroxyquinone (4.5g, 31.7mmoles) reduction under a hydrogen atmosphere and palladium metal catalyst yielded a crude product (4.36g, 97%). HPLC analyses gave three peaks at retention times 4.10 minutes (~50%), 4.28 minutes (~8%) and 4.46 minutes (~40%). These retention times corresponded to *myo*-inositol, *epi*-

inositol and *cis*-inositol respectively, as was confirmed by running standard inositols. The most difficult task in this exercise was to separate and purify *cis*-inositol using Dowex resin, as suggested by Angyal, Odier and Tate (1995). Elution fractions, which were reported to contain pure *cis*-inositol, were in this exercise found to contain traces of *myo*-inositol. The earlier fractions (2.25g) contained *myo*-inositol (50%) and traces of other inositols.

Since *cis*-inositol was being recovered in small amounts in any one fraction (30mL) and usually not completely pure, (approximately 90% purity) other methods of purification were investigated.

#### **2.3.3.1 Isolation of *cis*-inositol via isopropylidenation**

Attempts were made to isolate *cis*-inositol by isopropylidenation in order to obtain it about 99% pure. This is because the previous chromatographic method used, usually gave a product contaminated with *myo*-inositol (33).

The crude hydrogenation product (2.5 g) was dried in a vacuum desiccator for 72 hours. The dried material was refluxed with dry acetone and *p*-toluenesulphonic acid (0.1g, 0.01 mmoles) for 24 hours. The isopropylidenation product was purified using silica gel chromatography column with ethyl acetate / petroleum spirit mixture as eluent using each mixture (100mL) in increasing polarity. The elution solvent mixtures were prepared as shown in Table 7.

**Table 7: Ethylacetate/petroleum spirit mixture ratios.**

Mixture	ethyl acetate (%)	Petroleum spirit (%)
1	0	100
2	5	95
3	10	90
4	15	85
5	20	80
6	25	75
7	30	70

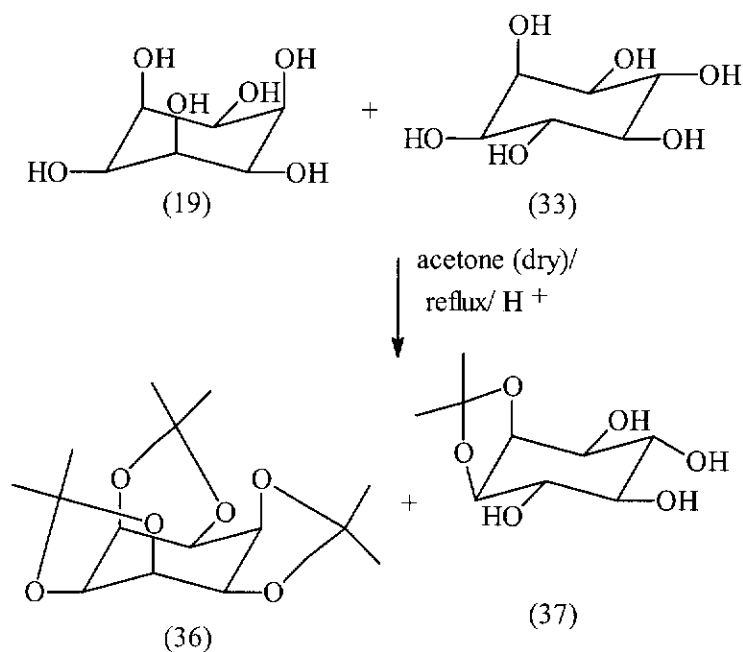


**Figure 20: Isopropylidenation of *cis*-inositol**

The eluted products were dried on a rotary evaporator to yield mixture 1 (0.3 g), mixture 2 (0.5 g), mixture 3 (0.8 g), mixture 4 (0.6 g), mixture 5 (0.1 g), mixture 6

(0.1 g) and in mixture 7 nothing was recovered. The recovered products were dissolved in deionised water (10 mL) and *p*-toluenesulphonic acid (0.05 g) was added and the mixtures were heated on a water bath (60-80 °C) for 5 hours then dried and recrystallised from methanol. Mixtures 1, 2 and 3 yielded white needle-like crystals with m.p. 220-226°C. <sup>13</sup>C NMR gave three signals, 74.42, 75.06 and 73.78 ppm and HPLC gave two retention time peaks, 4.46 (80%) and 4.40 (20%). The products from the polar mixtures gave numerous peaks in the <sup>13</sup>C NMR spectrum and HPLC retention time scale indicating that they were very impure. Initially it was anticipated that hydrolysis of structure 36 would give *cis*-inositol.

### 2.3.3.2 Purification of *cis*-inositol

It was observed that pure *cis*-inositol from the hydrogenation product would not recrystallise from a ethanol/water (3:1) mixture successfully, as reported by Angyal, Odier and Tate (1995). If, however, the solution was dried under vacuum, the residues showed the presence of *cis*-inositol and other inositols in minor amounts, both on HPLC and <sup>13</sup>C NMR analyses. In an effort to recover the pure *cis*-inositol, the inositol residues (1.03g) from column elution (fractions 15-45) were dissolved in methanol (10mL) with warming. Ethyl acetate (5mL) and petroleum spirit (40-70, 5mL) were mixed and the mixture added dropwise to the inositol solution until distinctly cloudy. The mixture was covered and let stand for five hours at room temperature (26°C). White needle crystals (0.25g, 25% yield, m.p. 311-314 ° C) formed and were collected by filtration. The crystals (5mg) were dissolved in deionised water (20mL) and analysed by HPLC. The HPLC chromatograms showed 100% *cis*-inositol at retention time 4.56 minutes and <sup>13</sup>C NMR spectra (69.38 and 75.70 ppm), Angyal and Odier (1982 ) reported 68.9 and 74.5 ppm.

### 2.3.4 Synthesis of *myo*-inositol carbonate

The first step in the synthesis of *myo*-inositol carbonate was to convert *myo*-inositol into its mono-orthoformate (figure 21), according to the procedure described by Kishi and Lee (1985). A colourless crystalline product was obtained.

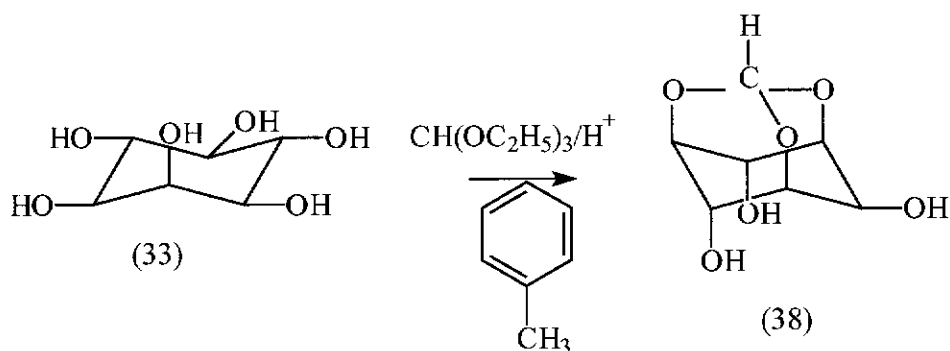


**Figure 21: Synthesis of *myo*-inositol mono-orthoformate**

Yield 94%, m.p. 298-301 °C,  $^{13}\text{C}$  NMR,  $\delta$  61.57, 67.80, 70.67, 75.86, and 103.27. Kishi and Lee (1985) reported yield 91%, m.p. 300-303 °C and  $^{13}\text{C}$  NMR ( $\delta$ : 61.0, 68.94, 70.47, 75.25 and 103.84).

#### 2.3.4.1 Purification of the orthoformate derivative

The *myo*-inositol mono-orthoformate was converted into the triacetate as described by Vasella *et al.* (1988), except that the mono-orthoformate (22.82g, 0.12moles) was added to a mixture of pyridine (50mL) and acetic anhydride (50mL) and was allowed to stand overnight, (Angyal, 1999). Ice water (150mL) was poured on to the solid product that resulted. The triacetate crystallised out and was filtered off on a Büchner funnel (41.03g, 0.12moles, m.p. 168-172 °C), (Kishi and Lee 1985, m.p. 173-174 °C),  $^{13}\text{C}$  NMR  $\delta$ : 21.29, 21.68, 63.77, 66.91, 68.28, 69.68, 103.11 and 169.90.

The triacetate (5.012g, 20mmoles) was dissolved in dry methanol (20mL) and sodium metal (0.005g, 0.2mmoles) was added and the mixture warmed over a water bath at 50 °C for 1 hour and the methanol removed under vacuum. Pure *myo*-inositolmono-orthoformate (3.15g, 0.02moles, 100% yield), was recrystallised from methanol (10 mL) m.p. 301-304 °C,  $^{13}\text{C}$  NMR  $\delta$ : 61.87, 69.20, 71.25, 76.34 and 104.16.

#### 2.3.4.2 Introduction of the silyl ether group

A solution of the mono-orthoformate (1.923g, 10mmoles) in dry DMF (20mL) was prepared. *tertiary*-Butyldimethylsilyl chloride (2.00g, 13mmoles) and imidazole (1.82g, 25mmoles) were dissolved in dry DMF (30mL) in a three necked flask under a nitrogen atmosphere. The solution was then cooled to 0 °C and by using a dropping funnel, the mono-orthoformate-*myo*-inositol solution was added to the flask dropwise over a period of 2.5 hours with continuous stirring. The reaction mixture was then stirred for 24 hours (figure 22).

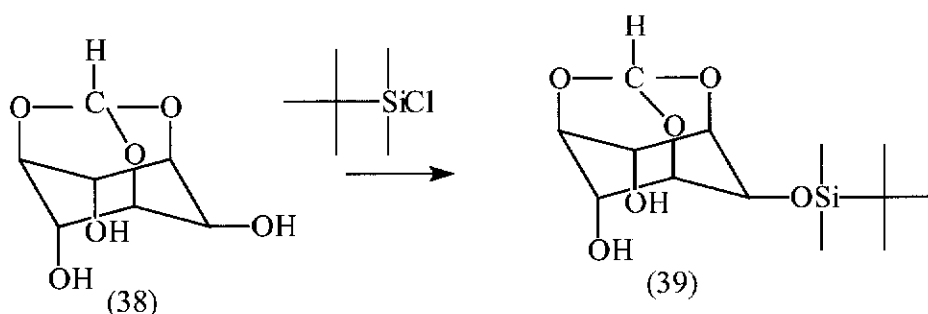
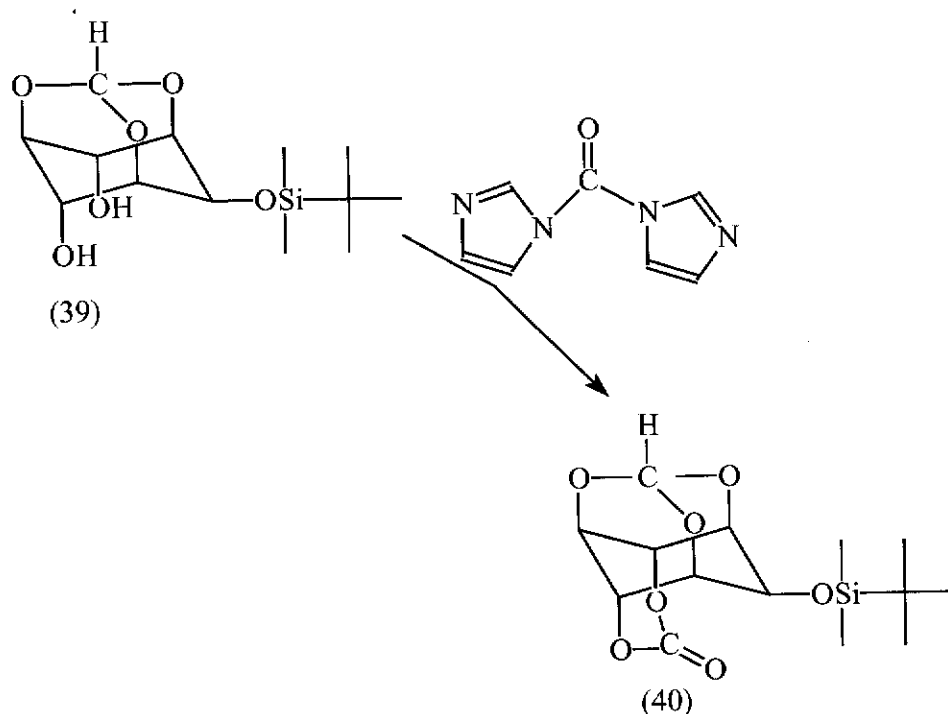


Figure 22: Synthesis of *tertiary*-butyldimethylsilylmono-orthoformate-*myo*-inositol

The silylated mono-orthoformate (39) (0.98g, 3mmoles, 30% yield, m.p. 176-179 °C (Kishi and Lee 1985, m.p. 179-181 °C, yield 48%) and  $^{13}\text{C}$  NMR  $\delta$ : -4.54, 19.12, 26.58, 61.47, 68.95, 69.55, 75.62 and 103.13) was collected and purified as described by Vasella *et al.* (1988). The spectroscopic data agree with that published by Kishi and Lee (1985).

#### 2.3.4.3 Formation of the protected *myo*-inositol carbonate

*tertiary*-Butyldimethylsilyl-mono-orthoformate-*myo*-inositol (39) (0.10g, 0.3mmoles) and *N,N*-carbonyldiimidazole (0.40g, 3mmoles) were dissolved with stirring in dry tetrahydrofuran (THF, 15mL), and stirred for 2 hours (figure 23).



**Figure 23: Synthesis of tertiary-butyldimethylsilylmono-orthoformate-myo-inositol carbonate**

Solutions of the silylated mono-orthoformate (39) (0.9g, 3mmoles) in dry THF (20mL) and *N,N*-carbonyldiimidazole (2.02g, 13mmoles) in dry THF (60 mL) were then added to the reaction mixture slowly from two separate dropping funnels. This was done in order to maintain the concentration levels of the reactants to a minimum because at high concentration levels side reactions tend to occur (Angyal 1999). The reaction mixture was continually stirred and kept under a nitrogen atmosphere. After the additions were completed, the reaction mixture was further stirred for 2.5 hours, then warmed up to 50°C and water was added dropwise initially. Addition of water continued until the solution became visibly cloudy (250mL), and was kept in a refrigerator for 12 hours. Glistening crystals (0.88g, 2.8mmoles) of the carbonate derivative (40) were collected and recrystallised from ethanol, m.p. 198-202 °C,  $^{13}\text{C}$  NMR  $\delta$ : -4.13, 19.05, 26.30, 60.70, 69.30, 70.90, 75.50, 102.60 and 182.5, IR 1755, 2928, 1390 and 1169  $\text{cm}^{-1}$ .

#### 2.3.4.4 Hydrolysis of substituents groups

a) The protected *myo*-inositol carbonate (40) (0.63g, 1.9mmoles) was dissolved in trifluoroacetic acid (60% solution in water) and stirred at room temperature for 24 hours (figure 24). The trifluoroacetic acid was removed by evaporation under reduced pressure and the residues (0.305g) recrystallised from hot methanol to give white crystals (0.269g, 43% yield, m.p. 187-191 ° C). The  $^{13}\text{C}$  NMR spectrum revealed that the hydrolysis resulted in other side reactions such that the end product was a mixture of a few products.

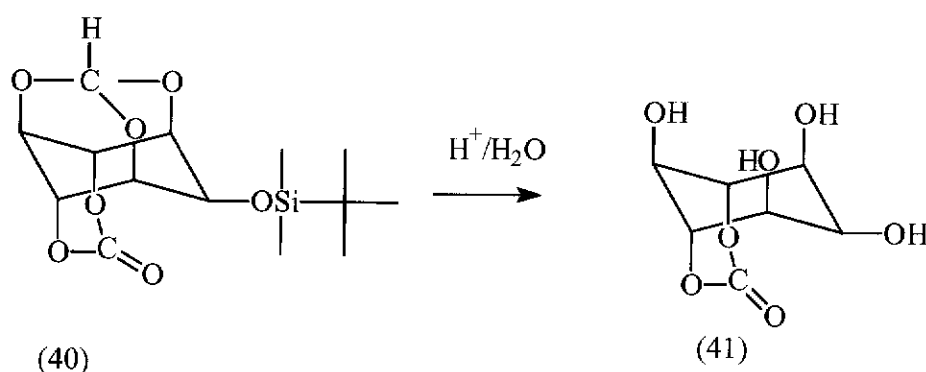


Figure 24: Hydrolysis of *tertiary*-butyldimethylsilyl-*myo*-inositol carbonate mono-orthoformate (40)

b) The protected *myo*-inositol carbonate (40) (0.63, 1.9mmoles) and trichloroacetic acid solution ( 60%, 20 mL) in water was stirred at room temperature for 24 hours (figure 24). Work up followed by recrystallisation from ethanol gave white crystals of *myo*-inositol carbonate (41) (0.335g, 1.6mmoles, 84% yield, m.p. = 204-209°C.  $^{13}\text{C}$  NMR  $\delta$  : 73.19, 74.24, 74.46, 76.41 and 184.57 ppm, IR 3385, 2922, 1757, 1447, 1147, 1050, 1001  $\text{cm}^{-1}$  (Angyal, 1999, m.p. 205-210 ° C).

## 2.4 PREPARATION OF SOLUTIONS FOR COORDINATION STUDIES

### 2.4.1 Ligand Solutions for NMR Studies

*myo*-Inositol and *epi*-inositol (0.504g, 2.8 mmoles) were dissolved in D<sub>2</sub>O (10mL) to give a concentration of 0.28 M. *cis*-Inositol (0.100g, 0.56 mmoles) was dissolved in D<sub>2</sub>O (10 mL) to give a concentration of 0.056 M and *myo*-inositol carbonate (0.505g, 2.8 mmoles) was dissolved in D<sub>2</sub>O (10 mL) to give a concentration of 0.28 M.

### 2.4.2 Cation solutions

Stock solutions of Ca<sup>2+</sup>, Al<sup>3+</sup>, Ga<sup>3+</sup>, Sm<sup>3+</sup> and La<sup>3+</sup> (0.28 M) were prepared in D<sub>2</sub>O (20mL) for coordination studies of *epi*-inositol, *myo*-inositol and *myo*-inositol carbonate. For coordination of *cis*-inositol stock solutions (0.028 M) of the above cations were prepared.

### 2.4.3 Sodium aluminate solution

Sodium hydroxide (1.00 g, 25 mmol) was dissolved in D<sub>2</sub>O (20 mL) and was heated to about 80 °C to give an NaOD solution. Clean aluminium wire (0.34 g, 12.5 mmol), was dissolved in the hot NaOD solution. The solution was then filtered through a 0.45 micron membrane filter to remove any solid particles. The filtrate was made up to 25 mL with hot D<sub>2</sub>O to give an aluminate solution of 0.50 M in 1 M NaOD.

### 2.4.4 NMR Complexation Ratios

The ratios in Table 8 were used for all NMR coordination studies undertaken. However, for HPLC the concentration of ligand was reduced to 0.0014M and equivalent cation concentration was added to achieve the ratios as shown in Table 8. The concentration of the ligand was maintained constant as the concentrations of cations were changed. This was achieved by fixing the volume to 1mL for all coordination ratios.

**Table 8: Coordination ratios**

Ligand (mmol)	Ligand volume (mL)	Cation volume ( $\mu$ L)	Cation (mmoles)	D <sub>2</sub> O make up volume to 1mL ( $\mu$ L)	Ratio L : M
0.14	0.5	0.0	0.000	500.0	1:0.00
0.14	0.5	62.5	0.035	437.5	1:0.25
0.14	0.5	125.0	0.070	375.0	1:0.50
0.14	0.5	187.5	0.105	312.5	1:0.75
0.14	0.5	250.0	0.140	250.0	1:1.00
0.14	0.5	312.5	0.175	187.5	1:1.25
0.14	0.5	375.0	0.210	125.0	1:1.50
0.14	0.5	437.5	0.245	62.5	1:1.75
0.14	0.5	500.0	0.280	0.0	1:2.00

## 2.5 THIN LAYER ION EXCHANGE CHROMATOGRAPHY

Ion exchange thin layer chromatography plates (Na<sup>+</sup> form) were rinsed with deionised water (200 mL) and soaked in hydrochloric acid (3M, 150 mL) for 24 hours and then rinsed with deionised water (250 mL). After air drying they were then soaked in aluminium, calcium, lanthanum or gallium solutions (0.56M) for 72 hours. Finally the plates were washed and rinsed with deionised water (300mL) and air dried. Solutions of *myo*-inositol, *myo*-inositol carbonate, *epi*-inositol and *cis*-inositol (10mg mL<sup>-1</sup> each) were prepared. Thin layer chromatographs of the inositols were concurrently developed on each cationic plate using deionised water as solvent. Spots were visualised by spraying the plates with sulphuric acid (10% in ethanol) and heating on a hot plate.

## Chapter 3 - Results and Discussion

### 3.1 SYNTHESSES

#### 3.1.1 Synthesis of *epi*-inositol

*epi*-Inositol was successfully synthesised although the yield was low. The loss of yield was apparently because the oxidation of *myo*-inositol to *epi*-inosose as described by Posternak, (1952) (figure 18) gave a yield of only 20% with most of the *myo*-inositol being over oxidised. As a future consideration, the yield may be improved by changing the oxidation step so that it can be better controlled. One possibility for improvement would be to use 35% nitric acid instead of the concentrated acid to effect milder oxidation conditions. If the yield of *epi*-inosose can be improved, it then follows that the overall yield of *epi*-inositol would improve too because the reduction of the *epi*-inosose produces *epi*-inositol in 80% yield.

#### 3.1.2 Synthesis of *cis*-inositol

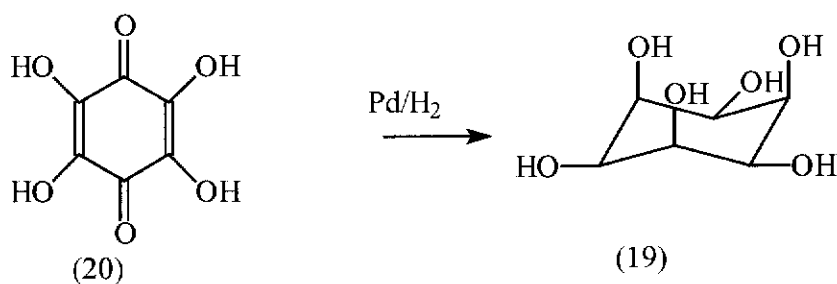


**Figure 25:** Synthesis of *cis*-inositol

The synthesis of *cis*-inositol was successfully undertaken but the experimental yield was between 5-8% pure product and 25% crude product, (Angyal, Odier and Tate, 1995, reported 30% yield pure product). The low yield was due to the loss of *cis*-inositol during the chromatographic separation. HPLC analysis showed that the first eluted fractions (1-14) had some *cis*-inositol mixed with other inositols, mainly *myo*-inositol (80-90%). This was not expected because according to Angyal, Odier and Tate, (1995) only eluted fractions 15- 45 (30mL each) were expected to contain pure *cis*-inositol while the other inositols were eluted in the first fourteen fractions. In this

work it was found that only 5-8% of *cis*-inositol was found in fractions 15- 45. The  $^{13}\text{C}$  NMR spectrum in  $\text{D}_2\text{O}$  of the purified product gave two signals assigned as C1,3,5 (69.38 ppm) and C2,4,6 (75.70 ppm). The results agreed with those reported by Angyal and Odier (1982), C1,3,5 (68.9 ppm) and C2,4,6 (74.5 ppm). It should be noted that recrystallisation of *cis*-inositol from water:ethanol (1:3) mixture as suggested by Angyal, Odier and Tate, (1995) did not work successfully. The *cis*-inositol did not recrystallise as expected. Hence, an ethylacetate/petroleum spirit mixture (1:1) was used to recrystallise the *cis*-inositol from methanol. This worked very well as the crystals came out of solution nicely within two to three hours.

Attempts were made to maximise the recovery of *cis*-inositol by isopropylidenation of the hydrogenation product. However, the extracted crystals gave three signals, 73.78, 74.42 and 75.06 ppm, in the  $^{13}\text{C}$  NMR spectra which indicated that the recovered product was not the expected *cis*-inositol. It is suspected that the reaction was refluxed for too long (24 hours), hence it is likely that the isopropylidenated product decomposed into a mixture of inositols. Although this initial attempt was not successful, the reaction methodology should be pursued further as it would provide a better method to isolate and purify *cis*-inositol.

### 3.1.3 Synthesis of *myo*-inositol carbonate

Since the synthesis and purification of *cis*-inositol proved to be tedious and low yielding, an alternative inositol was sought. The carbonate derivative of *myo*-inositol, (Angyal, 1999) locked in its unfavoured chair conformation, was prepared as it was expected to have the same coordination properties as *cis*-inositol.

The *myo*-inositol carbonate was synthesised and obtained pure, as shown by infrared and NMR data (section 2.3.4 ). The attachment of substituent groups was done fairly easily by following the procedures described by Vasella *et al.*, (1988) and Kishi and Lee (1985) and a yield of 50% was obtained. However, removal of the substituents groups by using trifluoroacetic acid solution (Angyal, 1999) was not successful and the resulting product contained many compounds, as was shown by  $^{13}\text{C}$  NMR spectral data. As a consequence of the forcing conditions used, possible side reactions may include hydrolysis of the carbonated moiety and/ or acid catalysed

dehydrations. Therefore the use of glacial acetic acid and trichloroacetic acid, both milder acids, were investigated to hydrolyse the substituent groups. The hydrolysis did not work with glacial acetic acid but the trichloroacetic acid did. The trichloroacetic acid was removed from the inositol by the addition of ethanol to the mixture until it became cloudy. The *myo*-inositol carbonate separated out and the  $^{13}\text{C}$  NMR spectrum gave five signals, (73.19, 74.24, 74.46, 76.41 and 184.57 ppm) assigned as C1,3, C2, C4,6, C5 and C=O respectively. The presence of the C=O group was confirmed by a sharp peak at  $1757\text{ cm}^{-1}$  in the infrared spectrum.

Surprisingly, the stability of the *myo*-inositol carbonate was observed to be limited because upon standing for about thirty days in a closed sample bottle, the product decomposed to *myo*-inositol, as shown by the  $^{13}\text{C}$  NMR spectrum (appendix 3). It is suspected that moisture was responsible for the decomposition but further observations are required to specifically establish the cause of the decomposition.

### 3.2 ASSIGNMENT OF THE $^{13}\text{C}$ RESONANCES OF THE INOSITOLS

The assignment of the  $^{13}\text{C}$  NMR signals for *epi*-inositol and *myo*-inositol was done by heteronuclear correlation analysis of the spectra as described by Silverstein and Webster (1998) (appendices 1.1 and 1.2). The assignment of the carbon signals in *cis*-inositol was not possible by heteronuclear correlation so assignments were based on the results obtained by Angyal and Odier. The *myo*-inositol carbonate had hydrolysed before the HECTOR spectrum was recorded. Therefore, for *myo*-inositol carbonate the assignment of carbon signals is tentative and the assignments for C1,3 and C4,6 may be interchanged; similarly C2 and C5 may also be interchanged. The results are given in Table 9 and compared with the assignments of Angyal and Odier (1982), and are in agreement with them.

**Table 9: Assignments of  $^{13}\text{C}$  NMR spectral resonances of inositols. (Angyal and Odier, 1982, shown in parenthesis)**

	<i>Epi</i> -inositol	<i>myo</i> -inositol	<i>cis</i> -inositol	<i>myo</i> -inositol carbonate
C1	73.8 (72.7)	73.2 (72.1)	69.4 (68.9)	73.2
C2	76.5 (75.5)	74.2 (73.2)	75.7 (74.5)	74.2
C3	68.8 (67.8)	73.2 (72.1)	69.4 (68.9)	73.2
C4	76.5 (75.5)	74.4 (73.4)	75.7 (74.5)	74.5
C5	73.8 (72.7)	76.4 (75.3)	69.4 (68.9)	76.4
C6	72.1 (71.1)	74.4 (73.4)	75.7 (74.5)	74.5
C=O				184.6

Literature values for *myo*-inositol carbonate are not available (Angyal 1999).

### 3.3 COORDINATION STUDIES

#### 3.3.1 Complexation studies by ion Exchange Chromatography

The ion exchange chromatography results for *epi*-inositol, *cis*-inositol, *myo*-inositol and *myo*-inositol carbonate (Table 10) showed a general trend of coordination by these inositols with calcium, aluminium and lanthanum.

**Table 10:  $R_f$  values of *cis*-inositol, *myo*-inositol, *myo*-inositol carbonate and *epi*-inositol on  $\text{Ca}^{2+}$ ,  $\text{Al}^{3+}$  and  $\text{La}^{3+}$  ion exchange plates.**

Inositols	$\text{Ca}^{2+}$	$\text{Al}^{3+}$	$\text{La}^{3+}$
<i>epi</i> -inositol	0.44	0.50	0.20
<i>myo</i> -inositol	0.90	0.51	0.70
<i>cis</i> -inositol	0.10	0.34	0.12
<i>myo</i> -inositol carbonate	0.60	0.60	0.70

Although the interpretation in terms of coordination modalities is not possible from these results, a general trend of complexation was established. The results show that *cis*-inositol binds very strongly with the calcium ion followed by lanthanum and

aluminium ions in that order. On the other hand, *epi*-inositol showed strong interaction with lanthanum ions followed by calcium and aluminium. *myo*-Inositol and *myo*-inositol carbonate showed only weak interactions with all the cations used. However, *myo*-inositol showed some preference for complexation with aluminium ions, whereas the coordination ability of *myo*-inositol carbonate seemed to be more or less the same for all the cations studied in this work. The results (Table 10) suggest that the coordination abilities of the inositols are *cis*-inositol > *epi*-inositol > *myo*-inositol carbonate ~ *myo*-inositol. The results of the ion exchange chromatography give a relative indication in terms of coordination strengths but do not provide information how the ligand binds to the cation and possible stoichiometry. Hence, it is not possible to suggest the mode of coordination and possible coordination sites on the basis of this data.

### 3.3.2 Complexation studies by HPLC

Attempts to study complexation of *epi*-inositol with calcium ions by HPLC were made and the results showed the possible formation of very stable complexes (appendix 2) which appeared to be directly proportional to the amount of calcium ions added. The HPLC chromatogram of *epi*-inositol without calcium ions gave one peak at retention time of 4.34 minutes and on addition of calcium ions (1:0.25, ligand:cation) the spectrum gave two peaks at retention times 3.30 and 4.32 minutes. The peak at 3.30 was broad and small but increased upon progressive addition of calcium ions and moved on the scale such that at the ratio of 1:1, ligand:cation, the peak was at retention time of 3.64 minutes and the peak due to *epi*-inositol had moved to retention time of 4.26 minutes. This trend continued until at the ratio of 1:2, ligand:cation, only one broad peak was observed at retention time of 3.98 minutes. However, a solution of calcium ions without *epi*-inositol under the same conditions gave a broad peak at retention time of ~3.0 minutes which suggests that the results were subject to interference, probably due to changes in refractive index of the solution on addition of the calcium ions, so that direct interpretation of the coordination modalities was in any event not possible, hence the exercise was not pursued further.

### 3.3.3 $^{13}\text{C}$ NMR Coordination studies of *epi*-inositol

The  $^{13}\text{C}$  NMR chemical shifts of *epi*-inositol were assigned on the basis of  $^1\text{H}$  and  $^{13}\text{C}$  NMR heteronuclear correlation (HETCOR) studies (appendix 1.1). The assignment is consistent with that of Angyal and Odier (1982 (Table 9). The coordination studies were carried out by observing  $^{13}\text{C}$  NMR chemical shift changes on sequential addition of cations. Positive chemical shift changes refer to downfield changes in chemical shift.

#### 3.3.3.1 Complexation of *epi*-inositol with calcium ions

The chemical shift of C2,4 showed a dramatic change upfield as calcium ions were added up to the ratio 1:1. Further addition after this ratio showed small chemical shift changes upfield indicating that a moderately stable complex had formed. In addition to this the signals for C2,4 and C3 broadened whereas the signals for C1,5 and C6 did not broaden, although their chemical shift changes were significant (figure 26). The increased shift change observed at 2:1  $\text{Ca}^{2+}$ : inositol ratio is surprising, as a second coordination site is not available on *epi*-inositol, and its origin is not clear.

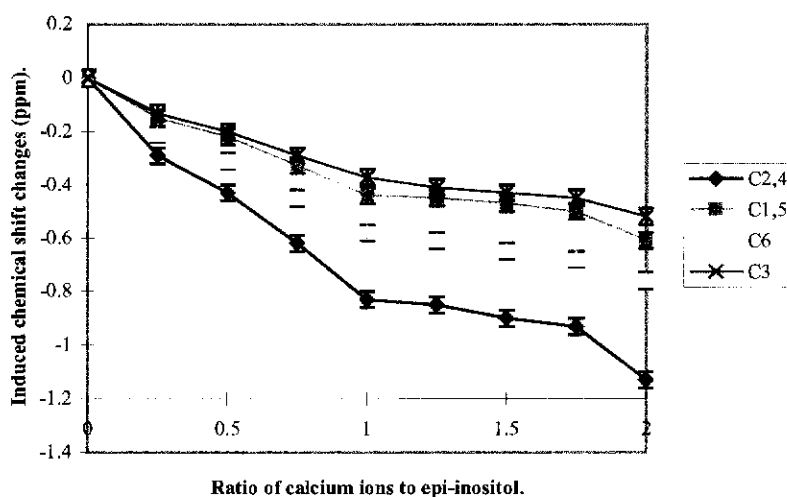
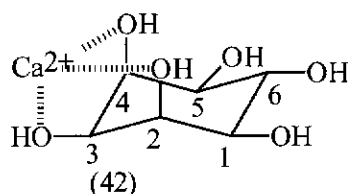


Figure 26:  $^{13}\text{C}$  NMR chemical shift changes of *epi*-inositol induced by calcium ions

These changes suggest that coordination most probably occurred at O-2, O-4 and O-3, an ax-eq-ax site of *epi*-inositol in its stable chair conformation (figure 27).



**Figure 27: Possible coordination of *epi*-inositol with calcium ions**

The surprising result is that C6 had the second largest chemical shift changes after C2,4. According to Angyal (1989), if the coordination mode is as shown in figure 27, then H3 should have the largest chemical shift changes which might suggest that C3 should similarly be affected, but this was not observed. However, the fact that the signals for C2,4 and C3 experienced both significant chemical shift changes and broadening, suggests that strong cation-ligand interactions occurred at O-2, O-3 and O-4. The signal broadening is considered to be part of the determining factor to indicate complexation because probably, the signals are broadened due to the equilibrium between the complexed and uncomplexed *epi*-inositol. Significant broadening would indicate moderately rapid exchange between the cation and the ligand, indicating complexation.

In the  $^1\text{H}$  NMR spectrum of *epi*-inositol in deuterium oxide, every hydrogen atom is distinguishable (Angyal and Hickman, 1975)(see Appendix 1). These authors reported that a large coupling constant of H6 ( $J_{5,6} = 10\text{Hz}$ ) defines the conformation of the chair form where H1, H5 and H6 are all in axial positions and that addition of barium, calcium, and strontium caused no changes in the coupling constant. This observation led them to conclude that *epi*-inositol complexes in its more stable chair form and not in the less stable triaxial form.

In this work a proton NMR spectrum of 1:1  $\text{Ca}^{2+}$ :*epi*-inositol also confirmed that the coupling constant of H6 ( $J_{1,6} = J_{5,6} = 10\text{Hz}$ ) remained constant and that *epi*-inositol

does not invert for coordination to occur. A possible rationale for the strong interaction at C6 may be due to either polar interactions between uncomplexed calcium ions in solution and O-6. It is very difficult, however, to understand why C6 is affected more than C1 and C5 as all of them are in the equatorial position of the stable chair conformation of *epi*-inositol and also that 2:1 ratio of  $\text{Ca}^{2+}$ :*epi*-inositol is unlikely as a second coordination site is not available.

### 3.3.3.2 Complexation of *epi*-inositol with aluminium ions

The magnitude of chemical shift changes as the amount of  $\text{Al}^{3+}$  ion was increased was quite small, particularly for aluminium:ligand ratios of less than 0.5:1 and only exceeded experimental error beyond this point (figure 28).

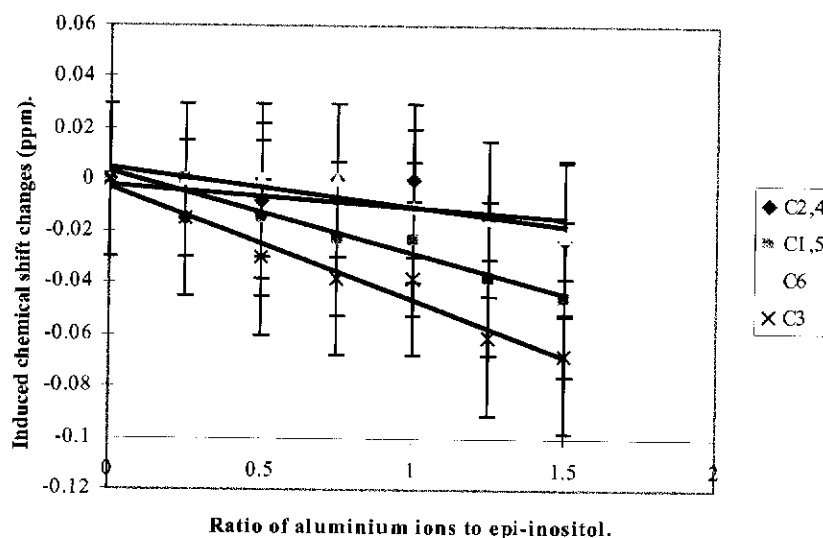
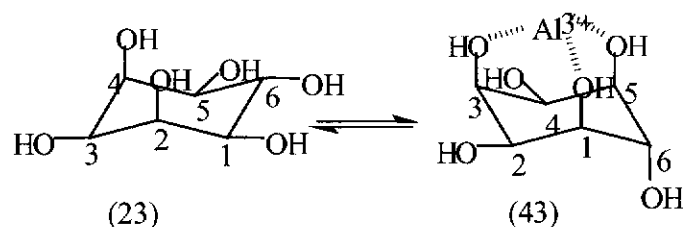


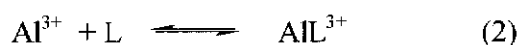
Figure 28:  $^{13}\text{C}$  NMR chemical shifts of *epi*-inositol on addition of aluminium ions

The trend lines in figure 28 indicate that there is a weak interaction with carbon atoms C1,5 and C3 shifting upfield suggesting that  $\text{Al}^{3+}$  ions coordinate weakly with *epi*-inositol at O-3, O-1 and O-5. and that the molecule experienced a ring inversion, as shown in figure 29.



**Figure 29:** Possible coordination of *epi*-inositol with aluminium ions

The suggested mode of coordination agrees with the observation made by Angyal (1989) that smaller ions coordinate better in the triaxial position. The ax-eq-ax position which involves O-2, O-3 and O-4 is ruled out in this case because very little effect is observed on C2,4. Another factor of note is that the  $\text{Al}^{3+}$  ion induced shifts appear to vary linearly (figure 28) suggesting that the chemical shift change is dependent on equilibrium dynamics (equation 2).



If the equilibrium constant is small then the addition of more  $\text{Al}^{3+}$  shifts the equilibrium to produce more complexed ligand as the  $\text{Al}^{3+}$ :*epi*-inositol ratio increases beyond 1.

### 3.3.3.3 Complexation of *epi*-inositol with gallium ions

The sequential addition of  $\text{Ga}^{3+}$  ions to the solution of *epi*-inositol in  $\text{D}_2\text{O}$  causes the greatest chemical shift changes on C3 followed by C1,5 (Figure 30). This suggests that interaction occurred at O-1, O-3 and O-5.

Although  $\text{Al}^{3+}$  and  $\text{Ga}^{3+}$  belong to group (III) of the periodic table, their coordination suggests there is a difference in that  $\text{Ga}^{3+}$  induces chemical shift changes twice those of  $\text{Al}^{3+}$ .

This indicates that the complexation stability of gallium-*epi*-inositol is greater than that of aluminium-*epi*-inositol. However, the trend of coordination displayed by  $\text{Ga}^{3+}$  ions is similar to that of  $\text{Al}^{3+}$  ions in that there is a ring inversion of the *epi*-inositol molecule in solution to create a triaxial site for complexation (figure 31).

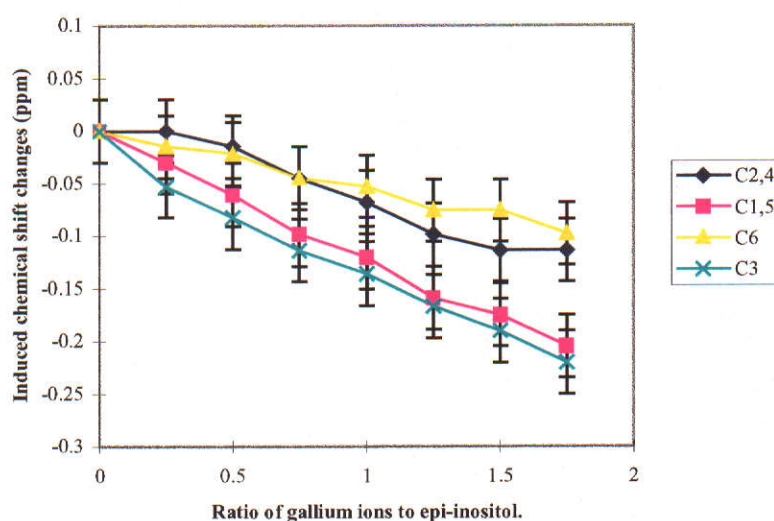


Figure 30:  $^{13}\text{C}$  NMR chemical shifts changes of *epi*-inositol induced by gallium ions

This difference can be explained as being due to the fact that  $\text{Ga}^{3+}$  ( $r_i = 60$  pm) is larger than  $\text{Al}^{3+}$  ( $r_i = 52$  pm) (Lee, 1983) and gallium ions are likely to fit better in the triaxial cavity than aluminium ions.

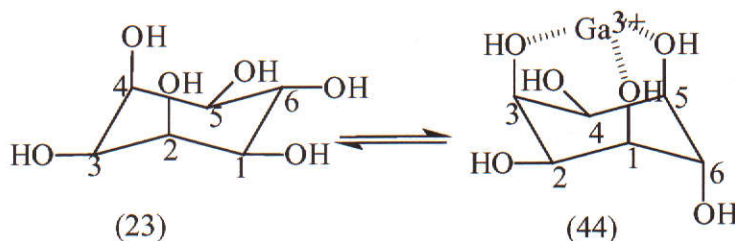


Figure 31: Possible coordination of *epi*-inositol with gallium ions

The level of chemical shift changes effected by  $\text{Ga}^{3+}$  show that *epi*-inositol does form reasonably stable complexes with  $\text{Ga}^{3+}$  ions and that coordination occurs at the triaxial site of its high energy conformation.

#### 3.3.3.4 Complexation of *epi*-inositol with lanthanum ions

Progressive additions of  $\text{La}^{3+}$  ions resulted in large chemical shift changes with signals for C1,5 and C6 shifting upfield (figure 32).

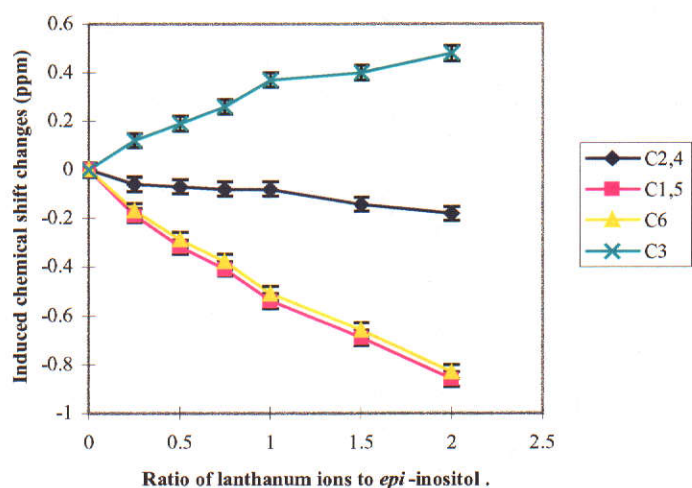
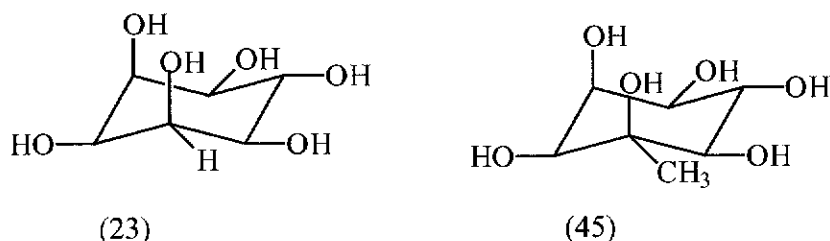


Figure 32:  $^{13}\text{C}$  NMR chemical shift changes of *epi*-inositol induced by lanthanum ions.

Also notable was the effect on C3 in that the shift was downfield suggesting that incremental addition of  $\text{La}^{3+}$  ions had a deshielding effect on C3. In the stable conformation of *epi*-inositol, C1,5 and C6 can not provide a favourable coordination site as neither a sequential ax-eq-ax nor a triaxial site for complexation are generated by them, even on ring inversion. The proton NMR spectrum of a 1:1 solution of *epi*-inositol: $\text{La}^{3+}$  showed that the coupling constant for H6 ( $J_{1,6} = J_{5,6} = 10\text{Hz}$ ) did not change suggesting that ring inversion had not occurred. The  $\text{La}^{3+}$  ion is large in size ( $r_i = 106\text{pm}$ , Greenwood and Earnshaw 1997) and according to the observations made by Dill and Carter (1989) this cation is suitable for ax-eq-ax coordination as cations of  $\sim 100\text{ pm}$  fit into the pocket provided by O-2, O-3, O-4 of *epi*-inositol. Cations with radii  $< 80\text{ pm}$  are too small for this binding pocket, but will readily fit into a 1, 3,5 triaxial pocket. This being the case, it is expected that *epi*-inositol should complex with  $\text{La}^{3+}$  in its stable chair conformation and it follows that the greatest chemical shift changes should be at C3 followed by C2,4. In this work C1,5 and C6 have the greatest chemical shift change, but as coordination is not possible at this site, the only possible tridentate sites to be considered are O-2, O-3, O-4 and O-1, O-3, O-5. If coordination occurs at O-1, O-3, O-5 (triaxial pocket) then one would expect a significant change in the spectrum and the chemical shift changes for C1,5 and C3 to be at least in the same direction. Therefore it is believed that coordination

most likely occurs at O-2, O-3, O-4 (the ax-eq-ax pocket) but to verify this  $^1\text{H}$  NMR was investigated.

Angyal and Greeves (1976) undertook a comprehensive  $^1\text{H}$  NMR study of lanthanide complexation with *epi*-inositol (23) and 2-C-methyl *epi*-inositol (45).



**Figure 33:** *epi*-Inositol and 2-C-methyl *epi*-inositol

They proposed that the chemical shift changes effected upon addition of lanthanides were due to three different mechanisms, through diamagnetic (always downfield), pseudocontact (dipolar interactions) and contact interactions. In their work they noted that the induced chemical shifts of H6 of *epi*-inositol and the methyl hydrogen atoms of 2-C-methyle*epi*-inositol with various cations were of the same sign and magnitudes as those due to pseudocontact interactions. Following this observation they concluded that in the spectrum of *epi*-inositol the induced chemical shift changes of H6 are due mainly to pseudocontact interactions.

In this work the  $^1\text{H}$  NMR induced chemical shifts were determined for a 1:1,  $\text{La}^{3+}$  : *epi*-inositol and a 1:1,  $\text{Sm}^{3+}$  : *epi*-inositol solution and the results (Table 11) compared with those obtained by Angyal and Greeves (1976).

**Table 11:**  $^1\text{H}$  NMR chemical shift changes of *epi*-inositol induced by lanthanum ions (Angyal and Greeves, 1976 shown in parenthesis)

Cation	$r_i$ (pm)	H1,5	H2,4	H3	H6
$\text{La}^{3+}$	101.6	0.04, (0.17)	0.11, (0.27)	0.11, (0.55)	0.09, (0.07)

These results show a similar trend of events although the magnitudes of induced chemical shift changes are slightly different. However, it is clear that both results show that the greatest effect is on H2,4 and H3 indicating that both ions,  $\text{La}^{3+}$  and  $\text{Sm}^{3+}$  most probably coordinate at O-2, O-3 and O-4 (figure 34).

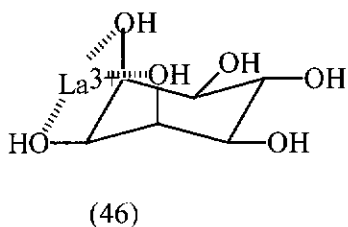


**Figure 34: epi-Inositol coordination with lanthanum ions**

The  $^1\text{H}$  and  $^{13}\text{C}$  NMR data seems contradictory and further investigation is required. The  $^1\text{H}$  NMR data suggests that the lanthanum ions coordinate at the ax-eq-ax site of *epi*-inositol (involving the hydroxyl groups on C2,4 and C3), while the  $^{13}\text{C}$  NMR data suggests coordination involving the hydroxyl groups on C1,5 and C6.

### 3.3.3.5 Complexation of *epi*-inositol with aluminate anions

In the  $^{13}\text{C}$  NMR spectrum of *epi*-inositol in deuterated sodium hydroxide ( $\text{NaOD}$ ) solution at approximately  $\text{pH} = 14$ , all signals shifted strongly downfield after addition of aluminate compared to the ligand solution in  $\text{D}_2\text{O}$  at  $\text{pH}$  near neutral. Sequential addition of aluminate anion to the solution of *epi*-inositol in  $\text{NaOD}$  then resulted in chemical shift changes upfield. The results indicate that C6 experienced the greatest chemical shift change as a function of aluminate concentration, such that it is possible to suggest an order of chemical shift changes as  $\text{C6} > \text{C3} \sim \text{C1,5} > \text{C2,4}$  (figure 35). This observation shows a likelihood of interaction at O-6 (moderate), O-3, O-1 and O-5. However, it was not clear why all the signals shifted dramatically after the addition of 0.25 equivalents of aluminate.

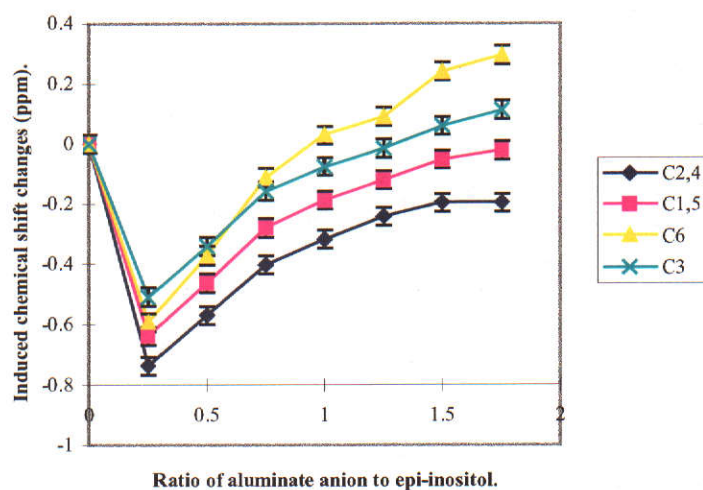


Figure 35:  $^{13}\text{C}$  NMR chemical shift changes of *epi*-inositol induced by aluminate anion

In the stable chair conformation of *epi*-insitol (figure 36), O-6 lies out of plane from the other O atoms and can not form a coordination site, even if the molecule is inverted, and it is therefore difficult to suggest a possible mode of coordination for it.

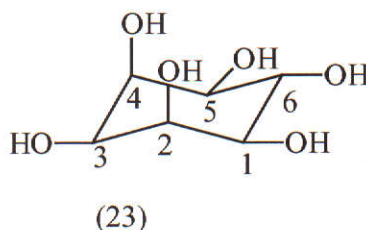
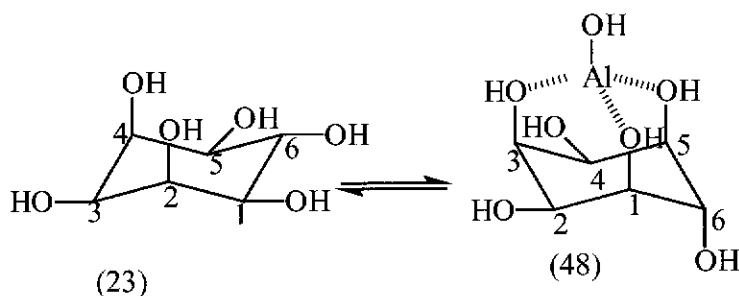


Figure 36: Stable chair conformation of *epi*-inositol

C3 lies directly opposite of the ax-eq-ax site of coordination comprising O-2, O-3 and O-4 and it is a carbon bearing an equatorial hydroxyl group such that if coordination occurred at this position, C3 in the structure (23) is expected to experience greater induced chemical shift changes than the other carbons. According to Angyal, (1989), carbons bearing an equatorial hydroxyl group are expected to experience greater induced chemical shift changes which in this case was not observed. In this case, because C1,5 also showed large chemical shift changes as aluminate anion was added, it is likely the anion coordinated at O-1, O-3 and O-5, suggesting a possibility of inversion of the *epi*-inositol molecule to structure (48)

which shows a triaxial site of O-1, O-3 and O-5 coordinated to aluminate species (figure 37).



**Figure 37: Possible inversion of *epi*-inositol**

It would appear therefore, that O-6 had a different interaction with the anion, one possibility is dipolar interaction with the aluminate ion. The aluminate species may have direct interaction with O-6, in which case C6 will experience changes in shielding resulting in the large induced chemical shift changes.

An important aspect observed is the fact that the aluminate anion induced greater induced chemical shift changes for C6 and C2,4 in *epi*-inositol  $^{13}\text{C}$  NMR spectra than does the aluminium ion in neutral solution. This suggests that pH plays a vital role to influence the coordination ability of a metal ion, in this case the aluminium ion. In effect these results are consistent with the observation made by Smith, Watling and Crew, (1996) that availability of organic polyols in the Bayer Process which operates under similar pH conditions, inhibits gibbsite crystallisation through surface poisoning or complexation.

### 3.3.4 $^{13}\text{C}$ NMR Complexation studies of *myo*-inositol

Angyal and Hickman (1975) and Angyal (1989) reported that the stereochemistry of *myo*-inositol hydroxy groups does not favour complexation because the molecule does not have an axial-equatorial-axial nor a triaxial arrangement of its hydroxy groups. For any coordination to occur, the complex must therefore provide sufficient energy to compensate the energy required to convert the molecule into its less favoured conformation. Angyal and Hickman (1975) reported that for this type of inversion to occur, about  $26 \text{ kJmol}^{-1}$  free energy must be overcome. It should be

pointed out that because of this large free energy requirement, *myo*-inositol is likely to form labile complexes. The unambiguous assignment of the  $^{13}\text{C}$  NMR spectrum of *myo*-inositol was achieved by analysis of the heteronuclear correlation spectrum (appendix 1.2) following the process described by Silverstein and Webster, (1998). The assignment is consistent with that of Angyal and Odier (1982).

### 3.3.4.1 Complexation of *myo*-inositol with calcium ions

The results show that calcium ions imparted significant chemical shift changes at the ratio 1:1 *myo*-inositol: calcium ions for C5 and C2. Further addition of calcium ions up to 1:1.5, *myo*-inositol: calcium ions did not produce any chemical shift changes (figure 38). This suggests that the optimal complexation ratio of *myo*-inositol: calcium ion system is 1:1 and that the complex is relatively stable (based on the relatively small change in chemical shift after a 1:1 ratio of metal ion to ligand). *Myo*-inositol can only act as a tridentate ligand when ring inversion has occurred (figure 39) which generates two possible coordination sites at the O1, O3, O5 and O1, O2, O3. Coordination at the 1,2,3 site should induce the greatest shift for C2 (Angyal, 1989) while at 1,3,5 one would expect a shift of all three carbons. Since the addition of calcium ions has the greatest effect on C2 and C5, it seems that coordination may be occur competitively at both sites.

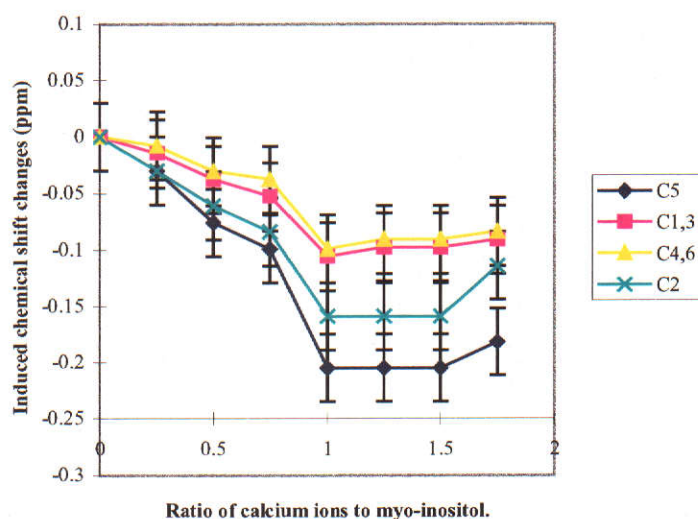
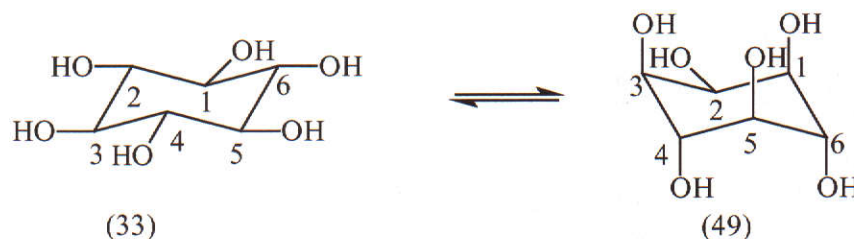


Figure 38:  $^{13}\text{C}$  NMR chemical shifts of *myo*-inositol induced by calcium ions

The *myo*-inositol:calcium coordination shows a possibility that the calcium ions complex at O-1, O-3 and O-5 with large chemical shift changes effected on C5 may be because it lies directly opposite to the coordination site. The large induced chemical shifts on C2 may be due to the fact that C2 lies directly opposite to the plane of coordination. This suggests that ring inversion occurred for coordination to take place (figure 39, structure 49).



**Figure 39:** Possible inversion of *myo*-inositol

### 3.3.4.2 Complexation of *myo*-inositol with aluminium ions

Not unexpectedly, a different pattern of results from that of calcium complexation is clearly displayed by the results for *myo*-inositol:aluminium ion interactions (figure 40). The results show that the interaction between aluminium ions and *myo*-inositol is weak because overall the induced chemical shift changes are small and do not reach a constant value. In this set of results one sees that the signal for C1,3 experienced the greatest chemical shift changes whereas for calcium it is the signal for C5. This demonstrates that calcium and aluminium coordinate to *myo*-inositol differently. However, it is clear that calcium ions bind to *myo*-inositol more strongly than aluminium ions because calcium ions induced larger chemical shift changes than aluminium ions.

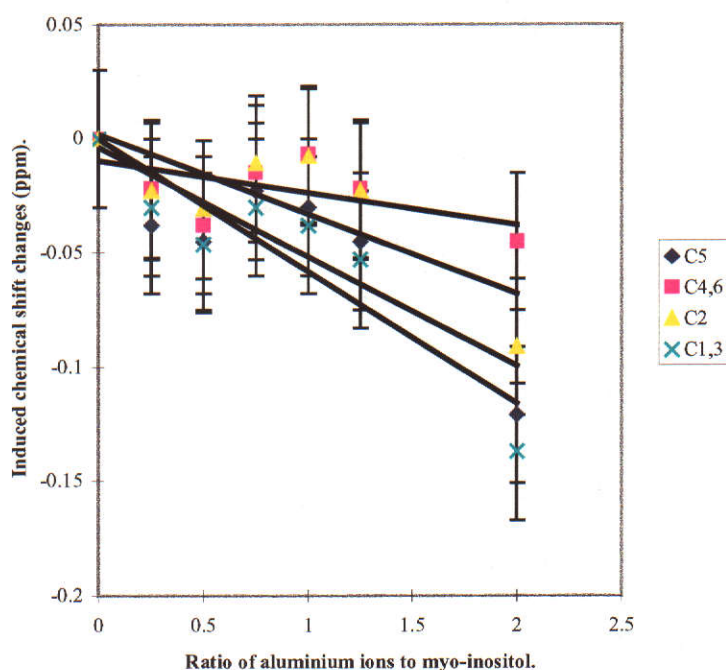


Figure 40:  $^{13}\text{C}$  NMR chemical shifts changes of *myo*-inositol induced by aluminium ions

The stronger interaction at C1,3 and C5 suggest that the aluminium ions weakly coordinate to O-1, O-3 and O-5. Although the chemical shift changes were not very large, it is postulated, that aluminium ions coordinated at the triaxial site of the less stable conformation of *myo*-inositol (49).

The difference in complexation between calcium and aluminium is due to the different sizes of the two ions. The small shift changes observed may be due to the ionic size of aluminium ion (52pm) which is too small to effectively coordinate at the triaxial pocket. This agrees with the observations made by Angyal, (1989) that triaxial sites coordinate better with cations with ionic radius of 60 pm.

### 3.3.4.3 Complexation of *myo*-inositol with Gallium ions

The values of chemical shift changes effected by gallium show that *myo*-inositol coordinates with gallium much better than aluminium but not as well as calcium ions. Significant induced chemical shift changes were observed for both signals of C1,3 and C5. At a 1:1 ratio the observed chemical shift changes are less than those observed for calcium ions. Further shift changes at ratios greater than 1:1 indicates that the  $\text{Ga}^{3+}$  ion complexation is weaker than the  $\text{Ca}^{2+}$  ion complexation (figure 41).

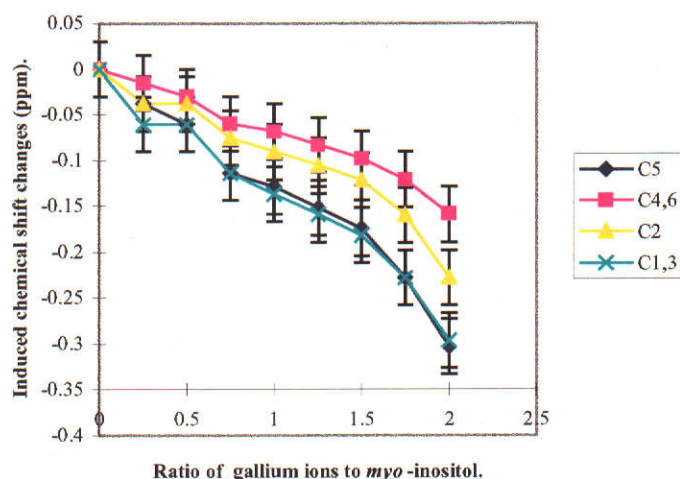


Figure 41:  $^{13}\text{C}$  NMR chemical shift changes of *myo*-inositol induced by gallium ions

These shift changes suggest that the *myo*-inositol molecule experienced a ring inversion to coordinate the gallium ions. The results in this case show that the effect on C1,3 and C5 is virtually the same. This observation agrees with that made by Angyal (1989) that smaller ions (60 pm) coordinate better at the triaxial site than larger ions such as calcium ion (100 pm). This fact seems not to be applicable to aluminium ions (52 pm) because, though it is a small ion and belongs to the same group as gallium (62 pm) on the periodic table, it has not displayed similar coordination abilities as gallium. The possible reason is that the aluminium ion is probably too small to fit the triaxial site for optimal coordination, such that the resulting complex of *myo*-inositol with aluminium ions is very weak.

These results suggest that cations with an ionic size of 60 pm coordinate better at the triaxial site than the ions with ionic size of 52 pm or 100 pm, indicating that for effective coordination at the triaxial site, ionic size plays a vital role. The fact that C1,3 and C5 experienced the same effect suggest that formation of a complex at the triaxial site by gallium ions causes little bond angle distortion for O-1, O-3 and O-5. This observation suggests that the ionic size of 60 pm is optimal for triaxial site coordination of *myo*-inositol. The charge of the cation did not appear to play a significant influence on the complexation in this case.

#### 3.3.4.4 Complexation of *myo*-inositol with lanthanum ions

The results of lanthanum:*myo*-inositol complexation show that C5 experienced the greatest chemical shift changes followed by C1,3 (figure 42).

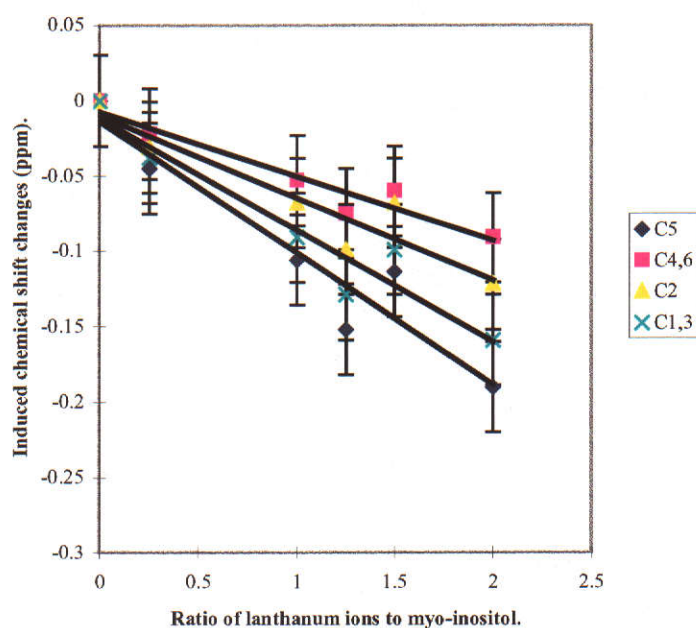
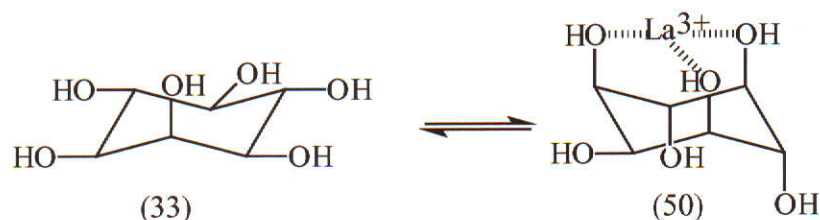


Figure 42:  $^{13}\text{C}$  NMR Chemical shift changes of *myo*-inositol induced by lanthanum ions

This suggests that lanthanum ions interacted with O-5, O-1 and O-3 such that there is a likelihood that lanthanum ions coordinated at these oxygen atoms (figure 43).



**Figure 43:** Possible coordination of *myo*-inositol with lanthanum ions

In terms of the magnitude of chemical shift change, lanthanum and calcium seem to have more or less the same effect on *myo*-inositol. The indications are that they both effect ring inversion and coordinate at the triaxial position. The induced chemical shift changes however, are small in magnitude compared to those induced by gallium but greater than those induced by aluminium ions, suggesting that its complexing strength lies in between these cations with a possible trend as  $\text{Al}^{3+} < \text{La}^{3+} < \text{Ga}^{3+}$  for *myo*-inositol complexation.

#### 3.3.4.5 Complexation of *myo*-inositol with aluminate anion

The aluminate anion does not effect large chemical shift changes on *myo*-inositol (figure 44). However, the signals for C5 and C1,3 showed slightly larger chemical shift changes than C2 and C4,6. In this case, therefore, it is possible to suggest that a very weak interaction occurred at C1,3 and C5 with C1, and C3 experiencing relatively greater effects than C5. The small upfield (positive) chemical shift changes may be a consequence at the interaction of the negative aluminate ion causing shielding of the carbon nuclei as opposed to the deshielding (positive shift) changes induced by cations.

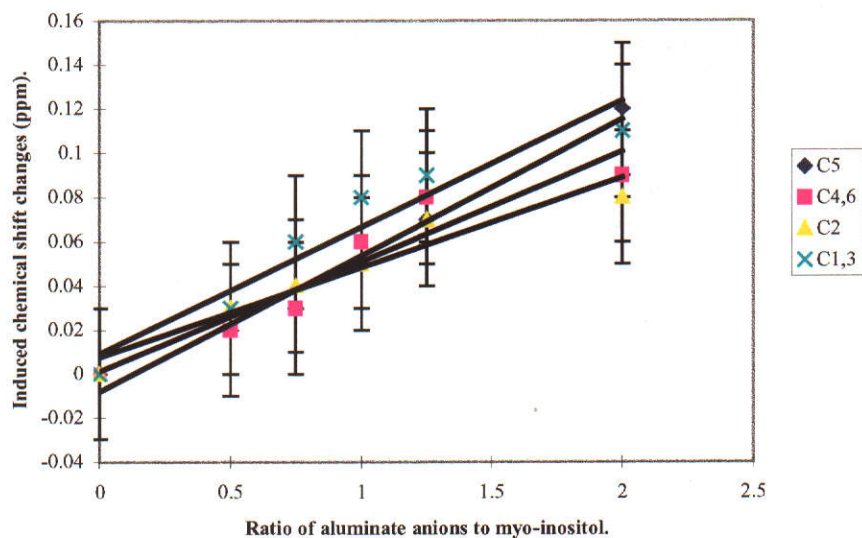


Figure 44:  $^{13}\text{C}$  NMR chemical shift changes of *myo*-inositol induced by aluminate anion

### 3.3.5 $^{13}\text{C}$ NMR Complexation Studies of *cis*-Inositol

Dill and Carter (1989) reported that *cis*-inositol binds more strongly to cations than the other inositols. The reason being that *cis*-inositol has four coordination sites, three ax-eq-ax and a triaxial site. In this work it was observed that the aluminate ion induced positive chemical shift changes. The reason for this is not well understood but perhaps it due to the fact that aluminate ion is negative and therefore would be expected to shield the carbon atoms whereas the cation would deshield them. It must also be noted that the purity of *cis*-inositol used was only 80-90%

#### 3.3.5.1 Coordination of *cis*-inositol with calcium ions

The chemical shift changes induced by  $\text{Ca}^{2+}$  ions, as can be seen from the figure 45, reveal that the signal for C2,4,6 had the greatest chemical shift effect. It was noted that the signal for C1,3,5 initially shifted slightly upfield up to the ratio 1:1, ligand:cation, but then, changed direction, shifting downfield. On the other hand, the signal for C2,4,6 shifted strongly upfield.

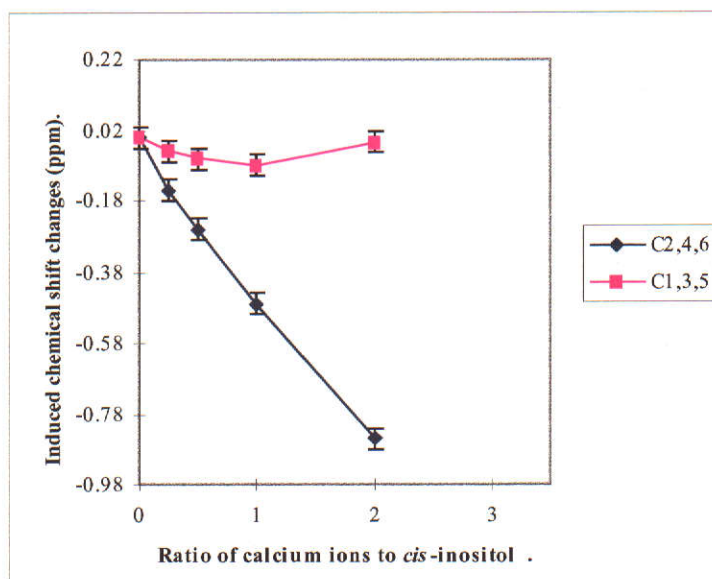


Figure 45:  $^{13}\text{C}$  NMR chemical shift changes of *cis*-inositol induced by calcium ions

It is likely therefore that the calcium ions coordinated, or at least had strong interactions with O-2, O-4 and O-6, suggesting a triaxial coordination (figure 46).

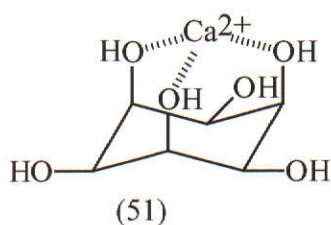


Figure 46: Possible coordination of *cis*-inositol with calcium ions

The  $\text{Ca}^{2+}$  ion ( $r_i = 100\text{pm}$ ) is very suitable for ax-eq-ax site coordination, according to Dill and Carter (1989). However, Angyal and Hickman (1975) observed that *cis*-inositol sometimes forms a 2:1 ligand:cation complex (figure 47). This phenomenon seems likely in this case because for the 2:1 complex, the molecule would prefer to coordinate via a triaxial site in order to minimise steric hindrance from the substituent groups. Dheu-Andries and Perez (1983), in their x-ray crystallography studies of calcium-sugar complexes, stated that calcium ions are in general coordinated to eight oxygen atoms in what they described as a “square-antiprismatic” arrangement (figure 16) and it is suspected that similar interactions occurred in this work (figure 47). However, octahedral complexes for instance calcium-EDTA complexes are also known.

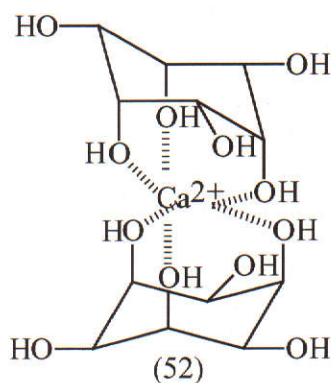


Figure 47: Possible *cis*-inositol:Ca<sup>2+</sup> 2:1 interaction

In this possibility, it is observed that O-2, O-4 and O-6 for both molecules are all directly involved whereas the equatorial oxygen atoms are not. In this case therefore the effect should be greatest on the signal for C2,4,6 as the results indicate, because all the three oxygen atoms have direct contact with the cation. The second reason is that the triaxial cavity is small for calcium ion such that for effective coordination, bond angle distortion is inevitable, hence, the greatest effects on C2,4 and 6. The possibility that the complexation may have occurred at an ax-eq-ax site involving O-4, O-5 and O-6 at the ratio of 1:1 ligand:cation (figure 48) is unlikely as this form of complex would give four signals in the <sup>13</sup>C NMR spectrum.

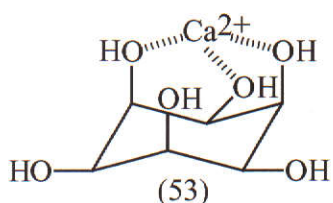


Figure 48: Possible 1:1 coordination of *cis*-inositol with calcium ions

Therefore the possible coordination sphere is as shown in figure 47, and is likely to be octahedral. From these results it is not possible to determine whether additional waters of coordination are present.

### 3.3.5.2 Complexation of *cis*-inositol with aluminium ions

A complexation study of *cis*-inositol with aluminium ions was carried out and the results show that very little interaction occurred especially at low ratios of  $\text{Al}^{3+}$  ion, (figure 49).

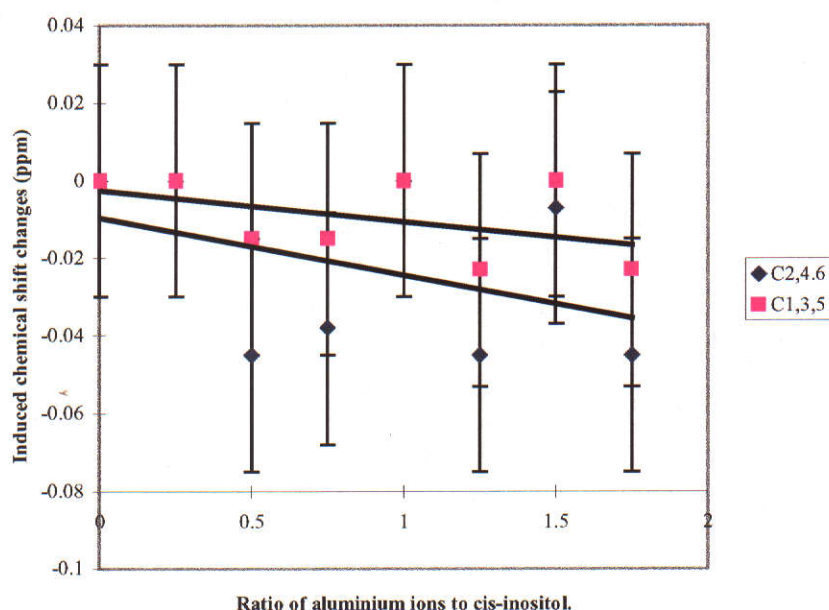
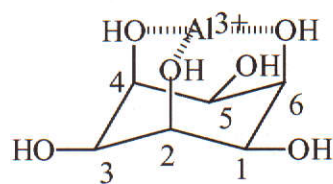


Figure 49:  $^{13}\text{C}$  NMR chemical shift changes of *cis*-inositol induced by aluminium ions

Although the aluminium ions effected little chemical shift changes, the results show that slightly larger induced chemical shift changes occurred for C2,4,6. It can therefore be said that  $\text{Al}^{3+}$  coordinated to O-2, O-4 and O-6. This suggests coordination at the triaxial site of *cis*-inositol as expected for a small cation ( $r_i = 52$  pm) (figure 50).



(54)

**Figure 50:** Possible coordination site of *cis*-inositol with  $\text{Al}^{3+}$  ion

It would seem, however, that the cation is weakly bound because the signals are affected mainly by the line broadening effect and very little chemical shift changes. The reason is likely due to the fact that the  $\text{Al}^{3+}$  ion is too small for effective coordination and bond angles of the oxygen atoms involved get strained due to distortions. The results agree with the observation made by Angyal (1989) and Dill and Carter (1989) that ion size is critical for effective coordination and that small ions prefer to coordinate in the triaxial cavity. A point worth noting is that the complexation of aluminium ions with *cis*-inositol seem to confirm that cations with ionic radii less than 52 pm would form very weak complexes at the triaxial site of *cis*-inositol. This suggests that the triaxial site requires a particular ionic size for effective coordination.

### 3.3.5.3 Complexation of *cis*-inositol with lanthanum ions

The results show that C1,3,5 had the greatest chemical shift changes overall although at the ratios 1:0.25, 1:0.5, and 1:0.75 the effect was the same on both signals, (figure 51). An interesting aspect of these results is that dramatic chemical shift changes occurred at the ratio 1:1 and that further addition of  $\text{La}^{3+}$  produced no significant chemical shift changes.

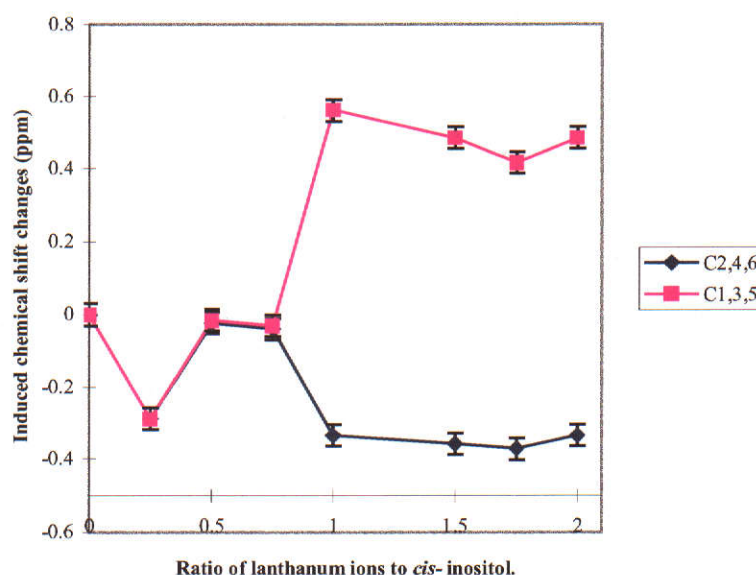


**Figure 51:**  $^{13}\text{C}$  NMR chemical shift changes of *cis*-inositol induced by lanthanum ions

These results suggest that the threshold of coordination for the *cis*-inositol: $\text{La}^{3+}$  system, is at the ratio 1:1 and that further addition of the cation impacted very little effect suggesting that a stable complex is formed. The surprising aspect in this study was the signals shifting in different directions, the signal for C1,3,5 was shifting down field whereas that for C2,4,6 was shifting upfield, suggesting that these carbon atoms were experiencing different effects. Further observations showed that the induced chemical shift changes for C1,3,5 were larger in magnitudes than for C2,4,6 (figure 51). One would therefore suggest that  $\text{La}^{3+}$  ions coordinated at the triaxial site of *cis*-inositol molecule (figure 52), such that at 1:1 ratio, there was moderately stable coordination. In which case addition of more cations would have very little effect as was the case for these results because the complex species (55) seems to have no more possible sites for coordination. Although lanthanum ion is a large cation (101.6 pm), it seems unexpectedly to prefer coordinating at the 1,3,5 triaxial site as coordination at an ax-eq-ax site would produce a complex with four magnetically inequivalent carbon atoms and hence four signals in the NMR spectrum. The reasons for this are not apparent.

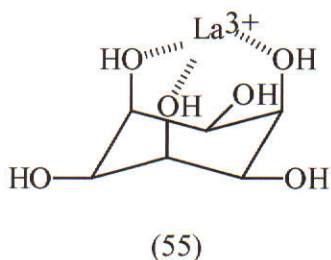


**Figure 52:** Possible coordination of *cis*-inositol with lanthanum ions

$\text{La}^{3+}$  ions had significant interaction at O-2, O-4 and O-6, as indicated by figure 51 and the shifts were upfield. This may be due to bond angle distortions which are likely when the suggested triaxial site coordinates the large lanthanum cation (101.6 pm).

### 3.3.6 $^{13}\text{C}$ NMR Complexation studies of *myo*-inositol carbonate

*myo*-Inositol carbonate (figure 24, structure 41) was used in this work because it is more readily prepared than *cis*-inositol and was expected to have coordination abilities similar to that of *cis*-inositol. This compound has only two complexation sites, an ax-eq-ax site and a triaxial site and it should be possible to compare coordination preference of cations with respect to these two sites. However, most of the cations studied with *myo*-inositol carbonate have shown preference to complex at the triaxial site as suggested by the magnitude of absolute values of observed induced chemical shift changes.

#### 3.3.6.1 Complexation of *myo*-inositol carbonate with calcium ions

In figure 53, the chemical shift data indicate that calcium ions imparted strong interaction with the *myo*-inositol carbonate in solution. Inspection of the figure shows that C1,3 and C5 experienced slightly greater chemical shift changes upfield than the other carbons.

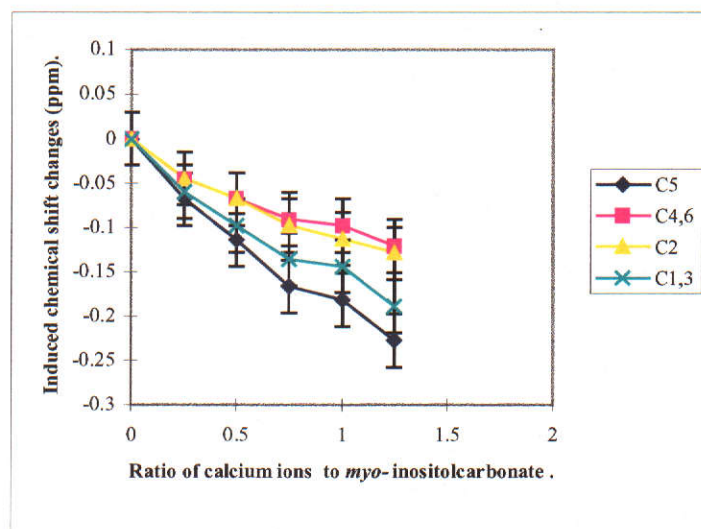


Figure 53:  $^{13}\text{C}$  NMR chemical shift changes of *myo*-inositol carbonate induced by calcium ions

Surprisingly the results seem to indicate that C4,6 and C2 were experiencing more or less the same interaction effect. However, since the effect was slightly stronger on C1,3,5 it was tentatively suggested that the calcium ions coordinate to O-1, O-3 and O-5 of *myo*-inositol carbonate (figure 54). The strong interaction may be due to the fact that calcium ions prefer to coordinate to multi-oxygen atoms of the ligand in solution as observed by Dheu-Andries and Perez, (1983). Therefore, similar interaction as predicted earlier (figure 47) might have occurred.

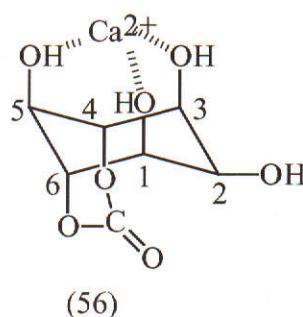
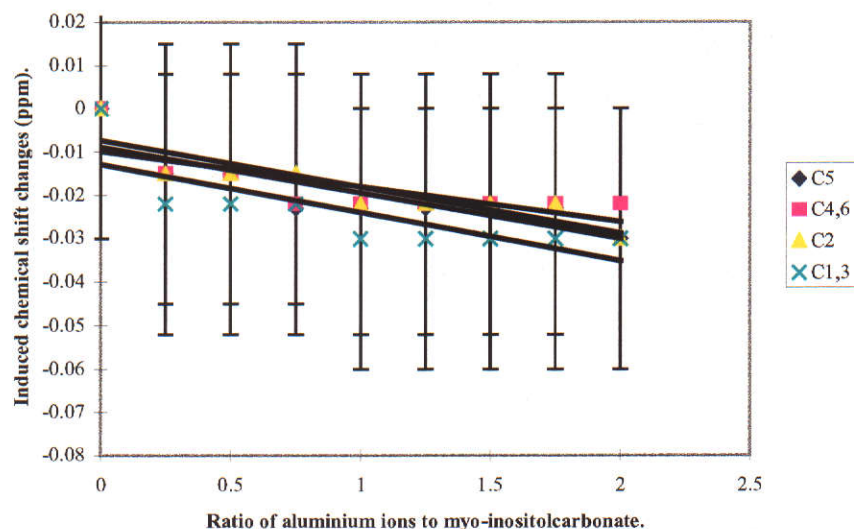


Figure 54: Possible coordination of *myo*-inositol carbonate with calcium ions

### 3.3.6.2 Complexation of *myo*-inositol carbonate with aluminium ions

The results indicate that there was very little interaction between the hydroxy groups of *myo*-inositol carbonate and the aluminium ions. However, the small effect

observed was reflected in C1,3 and C5 as the concentration of aluminium ions was increased (figure 55).



**Figure 55:**  $^{13}\text{C}$  NMR chemical shift changes of myo-inositol carbonate induced by aluminium ions

The results therefore suggest a weak interaction between *myo*-inositol carbonate and aluminium ions at O-1, O-3 and O-5. Aluminium ions seemed to form much weaker complexes, if any, with *myo*-inositol carbonate than with *myo*-inositol on the basis of the magnitude of induced chemical shift changes as observed in the two studies.

### 3.3.6.3 Complexation of *myo*-inositol carbonate with lanthanum ions

The study of *myo*-inositol carbonate coordination with lanthanum ions showed a different pattern of results from that of calcium ions. Experiments involving the coordination of lanthanum ions with other inositols have shown that sequential addition of lanthanum ions while maintaining the concentration of the ligand constant, resulted in progressive increase of the chemical shift changes. On the contrary, addition of lanthanum ions to the solution of *myo*-inositol carbonate showed only a slight effect on the chemical shift changes of  $^{13}\text{C}$  NMR spectra of *myo*-inositol carbonate (figure 56). The results suggest that although they are very

similar, the magnitudes of chemical shift changes seem to be in the order C1,3 > C5 > C2 > C4,6. Though increased lanthanum ion concentration showed little effect on the  $^{13}\text{C}$  NMR chemical shifts of *myo*-inositol carbonate, it is possible, however, to suggest that in solution *myo*-inositol carbonate may very weakly coordinate lanthanum ions at the triaxial site comprising O-1, O-3 and O-5. However, as C1,3 displayed slightly larger induced chemical shift changes, it is also possible that weak interactions occurred at O-1, O-2, and O-3, an axial-equatorial- axial site. Whatever is the case, the likely interactions in both cases were very weak as evidenced by small-induced chemical shift changes.

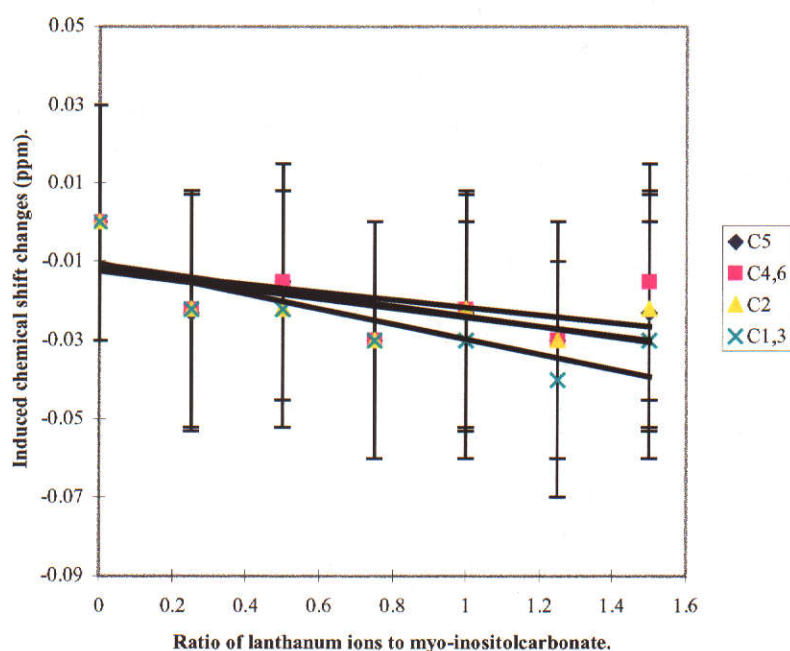


Figure 56:  $^{13}\text{C}$  NMR chemical shift changes of *myo*-inositol carbonate induced by lanthanum ions

#### 3.3.6.4 Complexation of *myo*-inositol carbonate with samarium ions

Addition of samarium ions to the solution of *myo*-inositol carbonate also resulted in very small chemical shift changes (figure 57). Generally the results seem to suggest that samarium ions ( $r_i = 96 \text{ pm}$ ), formed very weak complexes with the *myo*-inositol carbonate in solution. However, according to the results, one sees that the order in

magnitude of the effected chemical shift changes is  $C1,3 > C5 > C6 > C2,4$  indicating that possibly a weak interaction occurred at O-1, O-3 and O-5 (figure 58).

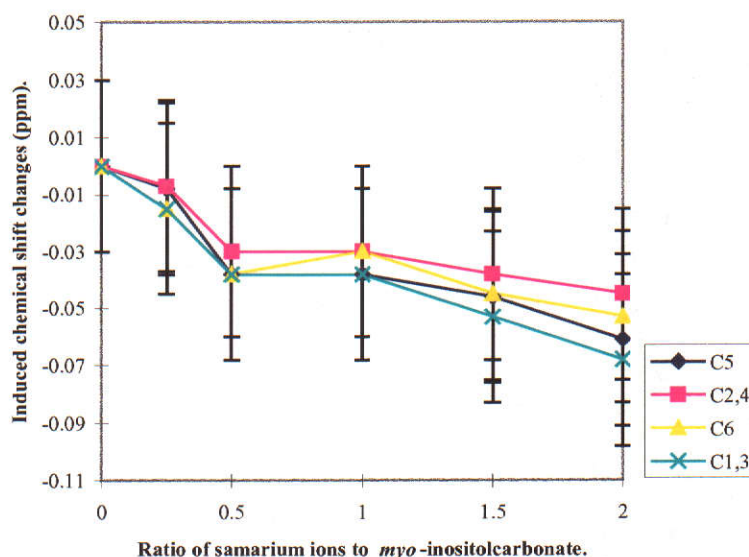


Figure 57:  $^{13}\text{C}$  NMR chemical shift changes of *myo*-inositol carbonate induced by samarium ions

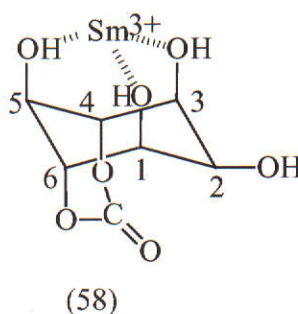


Figure 58: Possible coordination site of *myo*-inositol carbonate with  $\text{Sm}^{3+}$  ions

The complexation studies of aluminium, calcium, lanthanum and samarium ions with *myo*-inositol carbonate showed that only calcium ions effected a strong interaction with *myo*-inositol carbonate. However, all the four cations have shown a similar trend of coordination, effecting interactions on C1,3 and C5 suggesting coordination at the triaxial site of *myo*-inositol carbonate. The reason for calcium ions interacting relatively strong with the ligand is not clear but the multi-oxygen

atoms coordination preference of calcium ions in solution as observed by Dheu-Andreies and Perez (1983) may be one reason.

### 3.4 SUMMARY OF COORDINATION STUDIES BY $^{13}\text{C}$ NMR SPECTROSCOPY.

It should be pointed out that not many studies were done for *cis*-inositol because of a lack of sample, whereas the complexation of *myo*-inositol:samarium ions was not done because binding abilities of *myo*-inositol seemed to be weak in comparison with the other cations similar to  $\text{Sm}^{3+}$ . *myo*-Inositol carbonate-gallium complexation was not done because the *myo*-inositol carbonate sample had hydrolysed and due to time constraints another sample could not be made. The *myo*-inositol carbonate is base sensitive; hence, coordination studies with aluminate ions were not possible.

### 3.5 TRENDS OF POSSIBLE COMPLEXATION SITES.

Table 12 shows summary of the possible complexation sites of the inositols as has been observed in this work.

**Table 12: Possible complexation sites of inositols**

Inositol	$\text{Ca}^{2+}$	$\text{Al}^{3+}$	$\text{Ga}^{3+}$	$\text{La}^{3+}$	$\text{Sm}^{3+}$	$\text{Al}(\text{OH})_4$
<i>epi</i> -inositol	a-e-a (s)	ta (w)	ta (m)	a-e-a (s)	a-e-a (s)	ta (s)
<i>myo</i> -inositol	ta (m)	ta (w)	ta (m)	ta (w)	-	ta (w)
<i>cis</i> -inositol	ta (s)	ta (w)	-	ta (s)	-	-
<i>myo</i> -insitol carbonate	ta (m)	ta (w)	-	ta (w)	ta (w)	-

Where: a-e-a denotes axial-equatorial-axial.  
ta denotes triaxial  
w denotes weak,  
m denotes medium and  
s denotes strong.

The results seem to show that coordination of cations by *epi*-inositol can occur through both ax-eq-ax and triaxial sites. Cations with large ionic size have shown preference to ax-eq-ax sites whereas cations with small ionic size less than 80 pm seem to prefer triaxial sites for *epi*-inositol and *cis*-inositol although calcium (100 pm) and lanthanum (101.6 pm) have shown triaxial coordination. The summarised results, on the other hand show that *myo*-inositol and *myo*-inositol carbonate use the triaxial site to bind all of the cations studied in this work.

## CHAPTER 4 - CONCLUSIONS

This work has established that synthesis of *cis*-inositol by reduction of tetrahydroxybenzoquinone yields a mixture of inositols of which *myo*-inositol is the major component. Separation of the inositols into their pure form is the most difficult part of the synthesis. This is because the chromatographic separation technique has shown that some fractions still yield mixtures of inositols such that only between 5-8% of the product was pure *cis*-inositol.

Synthesis of *epi*-inositol, on the other hand, was successfully carried out with a 10% yield and the product was shown to be pure by NMR spectroscopy and HPLC analysis. However, the important aspect of this synthesis was that the *epi*-inositol was being obtained pure very easily.

The synthesis of *myo*-inositol carbonate was also carried out successfully and yielded 34% of the pure product, as confirmed by NMR and infrared spectroscopic analysis. *myo*-Inositol carbonate was synthesised because it has two possible coordination sites, ax-eq-ax and triaxial and it was anticipated to have a coordination ability similar to that of *cis*-inositol. A point worth noting is that this product appears to be sensitive to moisture because after standing for some time, the carbonate signal did not show on the  $^{13}\text{C}$  NMR spectrum indicating that it had undergone hydrolysis.

However, the  $^{13}\text{C}$  NMR coordination experiments indicated that it coordinated strongly only with calcium ions, but not with aluminium, lanthanum, and samarium ions. The coordination mechanism of calcium in this case is not well understood. However, it is postulated that calcium ions coordinate in a 2:1 fashion, ligand: cation (structure 52) as suggested by Dheu-Andrries, and Perez, (1983). This may be the reason why significant induced chemical shift changes were observed.

Generally it has been observed that *cis*-inositol binds strongly with calcium, lanthanum and gallium but weakly with aluminium ions both in solution and on ion exchange plates. This observation applies to *epi*-inositol but not *myo*-inositol which

coordinated better with gallium ions after a ring inversion, as indicated by NMR spectroscopy complexation studies.

NMR spectroscopy complexation studies showed that the ionic size of the cation plays a vital role for effective complexation. Aluminium ions ( $r_i = 52 \text{ pm}$ ) at near neutral pH show poor interaction with the inositols. On the other hand, gallium ions ( $r_i = 60 \text{ pm}$ ) have shown considerably stronger interactions under the same conditions. This difference is best explained as due to different ionic radii because both ions belong to the same group (III) of the periodic table and carry the same ionic charge.

Complexation studies of *epi*-inositol revealed that *epi*-inositol complexes cations with ionic size greater than  $80 \text{ pm}$  at the ax-eq-ax site whereas small ions are complexed at the triaxial site. Among the cations studied with *epi*-inositol, calcium, lanthanum and samarium have shown strong binding at the ax-eq-ax site of *epi*-inositol whereas gallium ions showed medium interaction at the triaxial site.

The aluminate ion displayed a strong interaction with *epi*-inositol in NaOD. The NMR data of the system *epi*-inositol:aluminate showed evidence of possible ring inversion of the *epi*-inositol molecule for coordination. This suggested that the aluminate anion coordinated at a triaxial site of O-1, O-3 and O-5. One surprising observation was that C6 experienced the greatest chemical shift changes despite the fact that in neither conformation of *epi*-inositol can O-6 form a favourable complexation site with the other hydroxy groups. The only explanation for this was that, probably, O-6 experienced a dipolar interaction with the aluminate anion resulting in large chemical shift changes, in addition to its change in position on inversion. In the final analysis one would suggest that aluminium ions complex better at high pH conditions where it exists as an anion, probably because the anion is slightly larger than the aluminium ion making it optimal for triaxial site complexation.

An attempted study of coordination by HPLC showed very interesting results, despite possible interference from refractive index changes of the solution which was

being detected by the refractive index detector used for this work. If it could be assumed that refractive index interference is negligible, the results showed formation of stable *epi*-inositol-calcium ion complexes. Again the chromatographic data seem to show that as calcium ions were being added, the relative concentration of the *epi*-inositol-calcium ion complex increased in a directly proportional manner. A clear conclusion from this exercise was not possible because the effect of the change in refractive index on the solution could not be accounted for.

It can be concluded that this work has demonstrated that  $^{13}\text{C}$  NMR spectroscopy is a very useful method for determining the extent of inositol-cation complexation in solution. Further, the results have shown that the chemical shift changes induced by cations in solutions of inositols provide a guide for identifying possible coordination configurations and therefore the hydroxy groups involved in the coordination.

Aluminium ions caused very small chemical shift changes in the  $^{13}\text{C}$  NMR spectrum of *epi*-inositol at pH near 7 whereas aluminate anions showed strong interaction with *epi*-inositol at pH about 14. This observation suggests that if inositols or similar compounds were present in the Bayer process, gibbsite crystallisation would be inhibited due to complexation with aluminate anion and that tridentate complexation is likely to be the most important binding mechanism.

The results of this work have satisfied the key objectives of the project in that *epi*-inositol and *cis*-inositol were synthesised successfully and coordination modalities of the inositols studied have been analysed.

## 4.2 FURTHER WORK

Additional work is required to improve the purification of *cis*-inositol which then will result in an improved yield. The isolation of *cis*-inositol using isopropylidenation needs to be investigated further.

Further work is also required to investigate closely the coordination studies of inositols by application of HPLC. A possible suggestion is that the suspected

complexes should be collected at the specific retention times and crystals of the complex grown. The grown crystals can then be studied by x-ray crystallography to determine coordination configurations of the inositols with various cations. The important part of this work would be to characterise and compare resultant complexes at different coordination ratios and this should include complexation of *myo*-inositol with samarium ions, *cis*-inositol with gallium, samarium and aluminate ions and *myo*-inositol carbonate with gallium ions.

## REFERENCES

- Akbulut, N and Balci, M. (1988). A new and stereospecific synthesis of cyclitols, (1,2,4/3), (1,2/3,4) and (1,3/2,4)-cyclohexanetetrols. *Journal of Organic Chemistry*, **53**, pp3338-3342.
- Aldrich (1990-1991). Catalogue/Handbook of fine chemicals, Aldrich Chemical Co. Inc. Milwaukee, pp1216.
- Angyal, S. J. (1989). Complexes of Metal Cations with Carbohydrates. *Advances in Carbohydrate Chemistry and Biochemistry*, **47**, pp2-35.
- Angyal, S. J. (1999). Personal Communications.
- Angyal, S. J. and Craig, D. C. (1993). Complex formation between Polyols and Rare Earth Cations. The Crystal Structure of galactitol $2\text{PrCl}_3 \cdot 14\text{H}_2\text{O}$ . *Carbohydrate Research*, **241**, pp1-8.
- Angyal, S. J. and Greeves, D. (1976). Complexes of Carbohydrates with Metal Cations. VII Lanthanides-induced shifts in the  $^1\text{H}$  NMR spectra of cyclitols. *Australian Journal of Chemistry*, **29**, pp1223-1330.
- Angyal, S. J., Greeves, D. and Littlemore, L. (1985). Complexes of Muellitol {1,3,5-Tri (3-methylbut-2-enyl)-scyllo-inositol} with Metal Cations. *Australian Journal of Chemistry*, **33**, pp1561-1566.
- Angyal, S. J., Greeves, D. and Mills, J. A. (1974). Complexes of Carbohydrates with Metal Cations. Conformation of Alditols in Aqueous Solution. *Australian Journal of Chemistry*, **27**, pp. 1447-1456.
- Angyal, S. J., Greeves, D. and Pickles, V. A. (1974). The Stereochemistry of Complex Formation of Polyols with Borate and Periodate Anions and with Metal Cations. *Carbohydrate Research*, **35**, pp165-173.
- Angyal, S. J. and Hickman, R. J. (1971). Cyclitols: A practical synthesis of *cis*-inositol. *Carbohydrate Research*, **20** pp97-104.
- Angyal, S. J. and Hickman, R. J. (1975). Complexes of carbohydrates with metal cations. IV Cyclitols. *Australian Journal of Chemistry*, **28**, pp1279-1287.
- Angyal, S. J., Littlemore, L. and Gorin, P. A. J. (1985). Lanthanide induced shifts in the  $^{13}\text{C}$  NMR Spectra of *epi*-inositol and Some Anhydrohexoses. The Anomalous

- Behaviour of the Heavy Lanthanides. *Australian Journal of Chemistry*, **38**, pp 411-417.
- Angyal, S. J. and Mills, J. A. (1979). Complexes of Carbohydrates With Metal Cations. XI Paper Electrophoresis of Polyols in Solutions of Calcium ions. *Australian Journal of Chemistry*, **32**, pp1993-2001.
- Angyal, S. J. and Mills, J. A. (1985). Complexes of Carbohydrates With Metal Cations. XIV Separation of Sugars and Alditols By Means of Their Lanthanum Complexes. *Australian Journal of Chemistry*, **38**, pp1279-1285.
- Angyal, S. J. and Odier, L. (1982). The  $^{13}\text{C}$  NMR Spectra of Inositols and Cyclohexanepentols: The Validity of Rules Correlating Chemical Shifts with Configuration. *Carbohydrate Research*, **100**, pp43-46.
- Angyal, S. J., Odier, L. and Tate, M. E. (1995). A Simple Synthesis of *cis*-inositol. *Carbohydrate Research*, **266**, pp143-146.
- ApSimon, J. (1973). *The Total Synthesis of Natural Products*, 1 pp66-70, John Wiley and Sons, Inc., New York.
- Beatie, J. K. and Kelso, M. T. (1981). Equilibrium and Dynamics of the Binding of Calcium to Sorbitol (D-Glucitol). *Australian Journal of Chemistry*, **34**, pp2563-2568.
- Burger, K. and Nagy, L. (1990). *Biocoordination Chemistry*, Ellis Horwood, Chichester, pp 236-272.
- Collins, P. M. and Ferrier, R. J. (1995). *Monosaccharides, Their Chemistry and Their Roles in Natural Products*, John Wiley and Sons, Chichester.
- Dill, K. and Carter, R. D. (1989). The Interactions of Metal Ions With Carbohydrates. *Advances in Carbohydrate Chemistry and Biochemistry*, 47 pp125-166.
- Dheu-Andries, M. L. and Perez, S., (1983). Geometrical Features of Calcium-Carbohydrate Interactions. *Carbohydrate Research*, **124**, pp324-332.
- Fatiad, A. J. and Sager, W. F. (1973). Tetrahydroxyquinone. Organic Synthesis Collective Volume V, pp1011-1012.

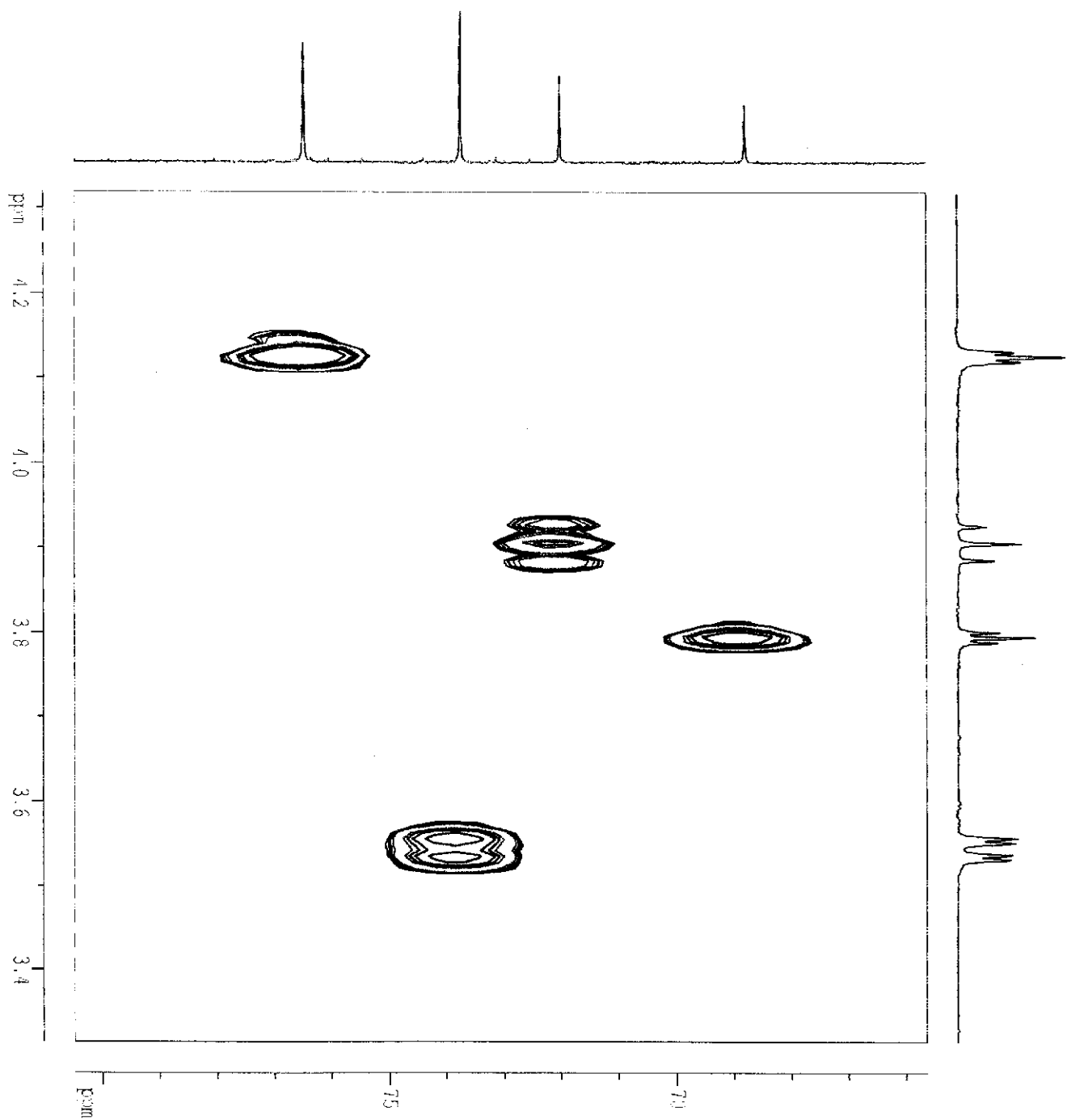
- Greenwood, N. N. and Earnshaw, A. (1997). *Chemistry of the elements*, 2<sup>nd</sup> ed., pp243-277, Butterworth-Heinemann, Oxford.
- Guthrie, R. D. and Honeyman, J. (1968). *An Introduction to the Chemistry of Carbohydrates*, 3<sup>rd</sup> ed., pp88-89, Clarendon Press, Oxford.
- Kishi, Y. and Lee, H.W. (1985). Synthesis of Mono and Unsymmetrical Bis Ortho Esters of Scyllo-inositol. *Journal of Organic Chemistry*, **50**, pp 4402-4404.
- Lee, J. D. (1983). *A New Concise Inorganic Chemistry*, 3<sup>rd</sup> ed, Van Nostrand Reinhold (UK), Berkshire.
- Lever, G. (1978). Identification of Organics in Bayer Liquor, *Light Metals*, pp 71-82.
- Painter, T. J. (1996). A Mnemonic for Inositols. *Journal of Chemical Education*, **73** (10), pp949-950.
- Posternak, T. (1952). *Myo-* and *DL-epi-*inosose. *Biochemical Preparations*, **2**, pp62-63.
- Power, G. P. (1991). The Impact and Control of Organic Compounds in the Extraction of Alumina from Bauxite', in Extractive Metallurgy Conference, Perth, pp. 337-344.
- Ollis, J, James, V. J., Angyal, S. J. and Pojer, P.M. (1978). An X-ray Crystallographic Study of D-Allopyranosyl-D-Allopyranoside.CaCl<sub>2</sub>.5H<sub>2</sub>O (A Pentadentate Complex). *Carbohydrate Research*, **60**, pp219-228.
- Silverstein, R.M. and Webster, F.X. (1998). *Spectrometric Identification of Organic Compounds*, 6<sup>th</sup> ed., John Wiley and Sons, New York, pp259.
- Smith, P. G., Watling, H. R. and Crew, P. (1996). The Effects of Model Organic Compounds on Gibbsite Crystallisation From Alkaline Aluminate Solutions: Polyols. *Colloids and Surfaces A: Physicochemical and Engineering Aspects*, **111**, pp119-130.
- Symons, M. C. R., Benbow, J. A. and Pelmore, H. (1984). Interaction Between Calcium Ions and Range of Monosaccharides Studied by Hydroxy-proton Resonance Spectroscopy. *Journal of the Chemical Society Faraday Transactions 1*, pp1999-2016.

- Tajmir-Riahi, H. A. (1983). Sugar Complexes With Calcium Ion: Infrared Spectra of Crystalline D-Glucuronic acid and its Calcium Complexes. *Carbohydrate Research*, **122**, pp241-248.
- Vasella, A., Baudin, G., Glanzer, B. I and Swaminathan, K. S. (1988). A Synthesis of 1D- and 1L-*myo*-inositol 1,3,4,5-Tetraphosphate. *Helvetica Chimica Acta*, **71** pp1367-1378.
- Veening, H. and Willeford, B. R. (1979). High Performance Liquid Chromatography In Organometallic and Coordination Chemistry. *Reviews in Inorganic Chemistry*, **1**, pp281-302.

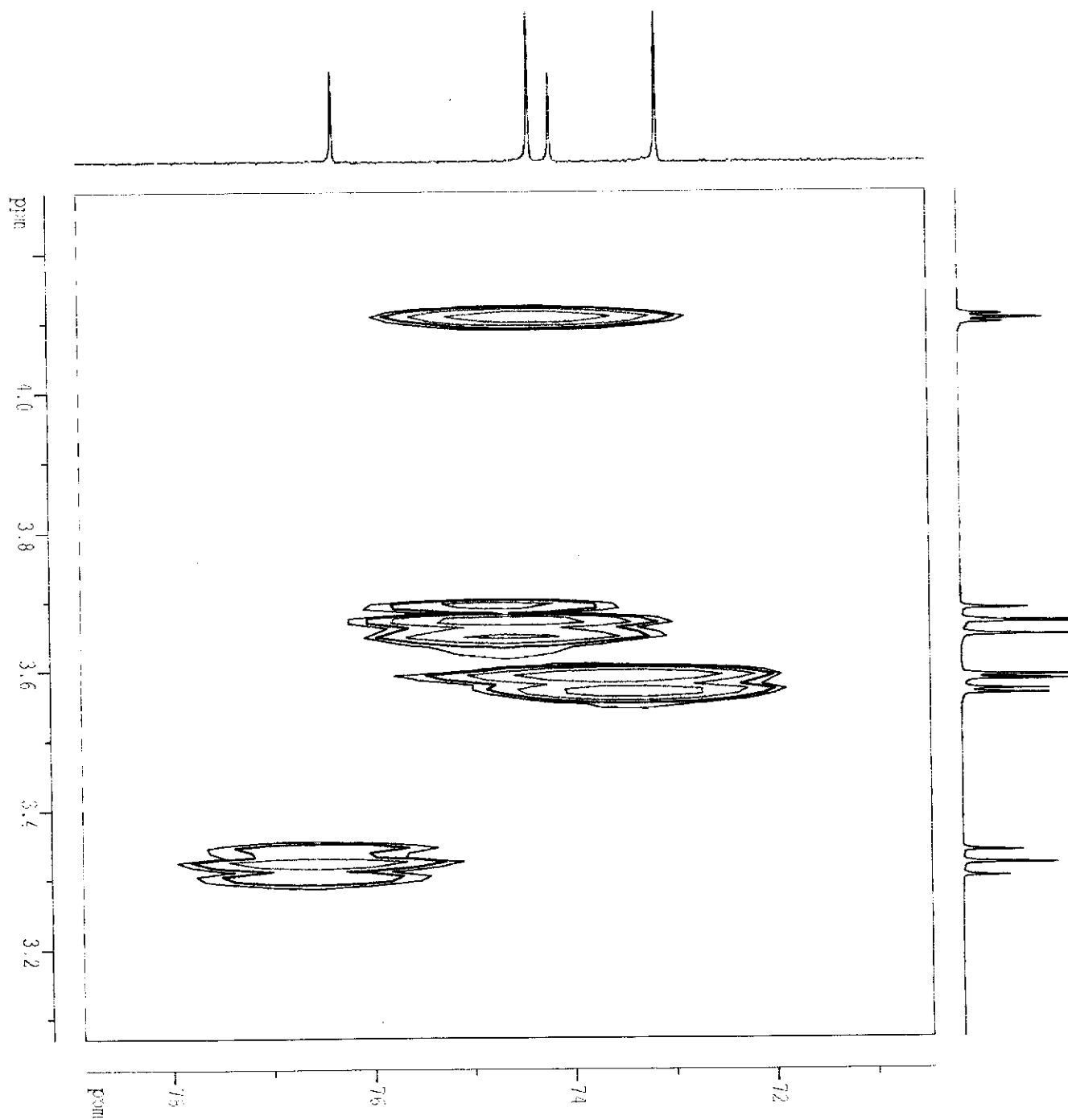
## APPENDICES

- Appendix 1.1 HECTOR spectrum of *epi*-inositol.
- Appendix 1.2 HECTOR spectrum of *myo*-inositol.
- Appendix 2.0 HPLC complexation studies of *epi*-inositol with calcium ions.
- Appendix 3.0  $^{13}\text{C}$  NMR spectrum of hydrolysed *myo*-inositol carbonate.

**Appendix 1.1 HETCOR spectrum of *epi*-inositol.**

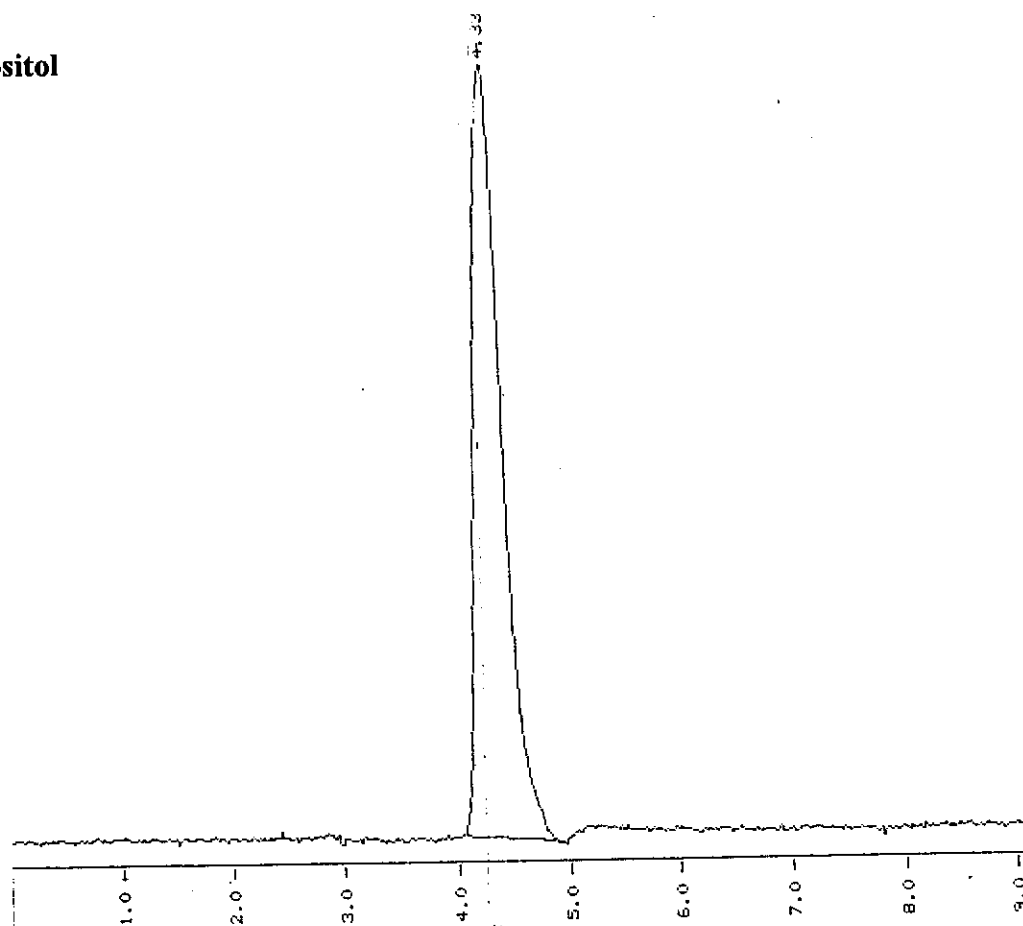


**Appendix 1.2 HETCOR spectrum of *myo*-inositol.**

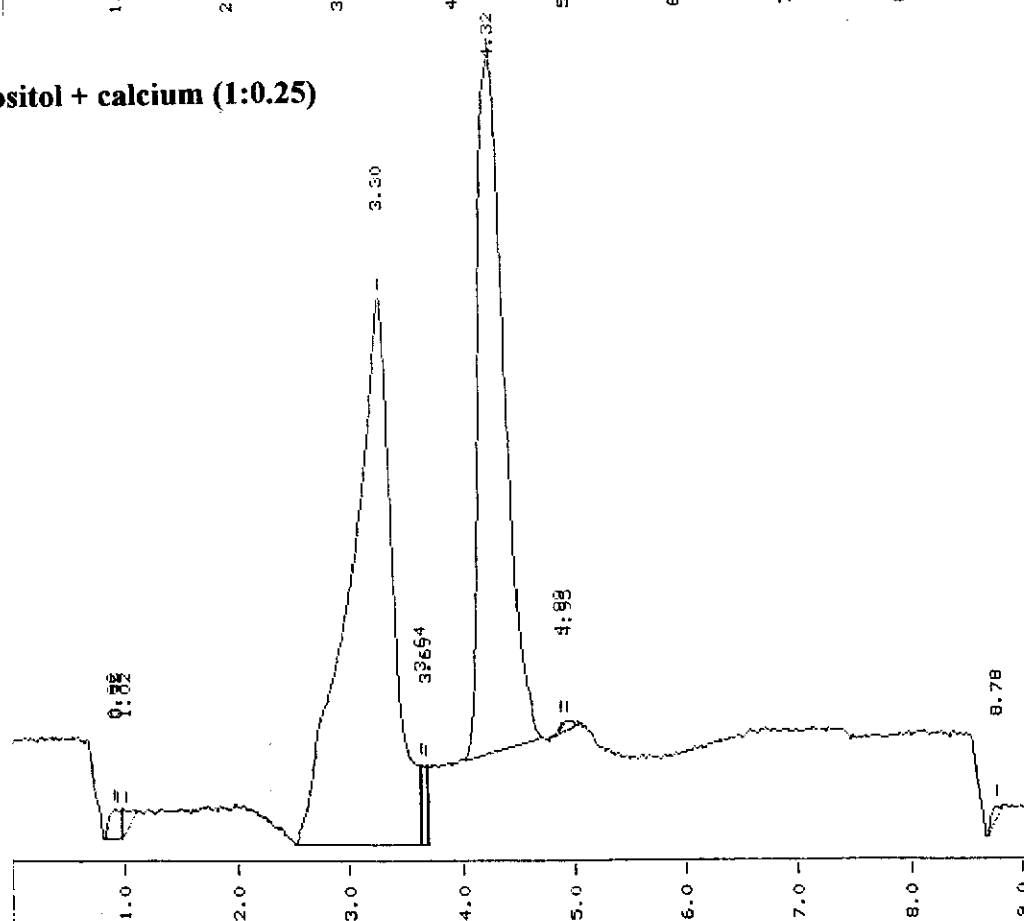


## Appendix 2.0 HPLC complexation studies of *epi*-inositol with calcium ions.

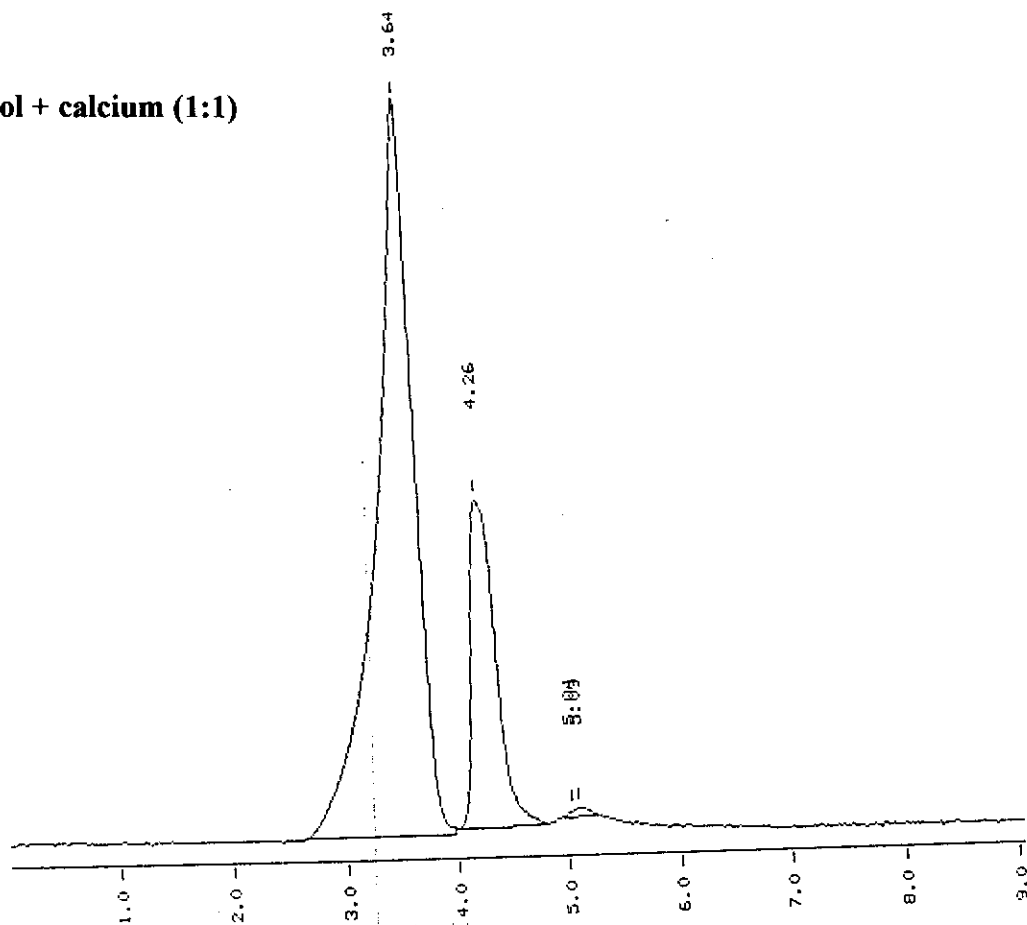
*epi*-inositol



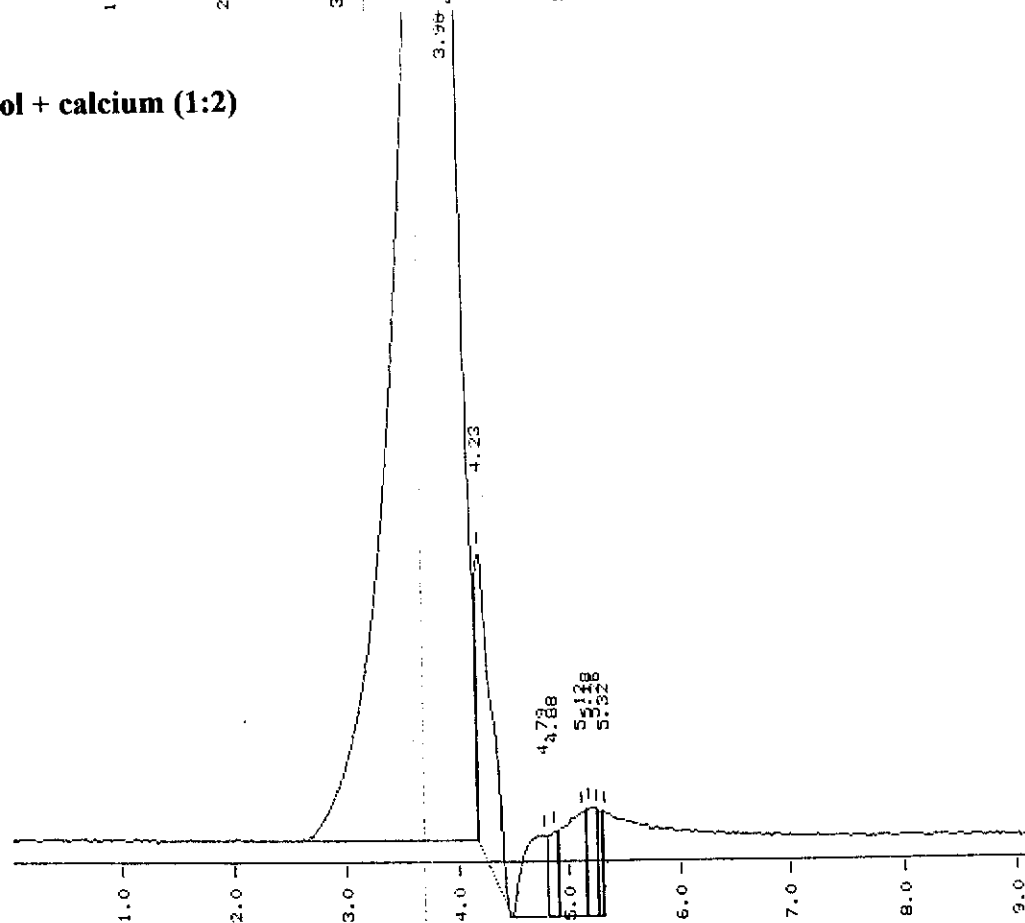
*epi*-inositol + calcium (1:0.25)



***epi*-inositol + calcium (1:1)**



***epi*-inositol + calcium (1:2)**



# Appendix 3 <sup>13</sup>C NMR spectrum of hydrolysed *myo*-inositolcarbonate.

Current Data Parameters  
NAME mm-myo-carb  
EXPNO 3  
PROCNO 1

F2 - Acquisition Parameters  
Date\_ 990217  
Time 10.30  
INSTRUM arx500  
PROBHD 5 mm Multinucl  
PULPROG zgpg30  
TD 65536  
SOLVENT CDCl3  
NS 800  
DS 4  
SWH 35714.285 Hz  
FIDRES 0.544957 Hz  
AQ 0.9175540 sec  
RG 32768  
RW 14.000 usec  
DE 20.00 usec  
TE 300.0 K  
D12 0.0000200 sec  
DL6 24.00 dB  
D1 1.00000000 sec  
CPDPRG waltz16  
P31 100.00 usec  
D11 0.0300000 sec  
DL5 19.00 dB  
P1 12.00 usec  
DE 20.00 usec  
SF01 125.772900 MHz  
NUCLEUS 13C

F2 - Processing parameters  
SI 65536  
SF 125.7592126 MHz  
WDW EM  
SSB 0  
LB 1.00 Hz  
GB 0  
PC 1.40

1D NMR plot parameters  
CX 20.00 cm  
F1P 220.000 ppm  
F1 27667.03 Hz  
F2P -10.000 ppm  
F2 -1257.59 Hz  
PPMCM 11.50000 ppm/cm  
HZCM 1446.23095 Hz/cm

76.3189  
74.3701  
74.1528  
73.0998

